

Finding a needle in a haystack: producing antimicrobial cutin-derived oligomers from tomato pomace

Rita Escórcio,¹ Artur Bento,¹ Ana S. Tomé,¹ Vanessa G. Correia,¹ Rúben Rodrigues,¹ Carlos J.S. Moreira,¹ Didier Marion,² Bénédicte Bakan,² Cristina Silva Pereira^{1,*}

¹ *Instituto de Tecnologia Química e Biológica António Xavier, Universidade Nova de Lisboa (ITQB NOVA), Av. da República, 2780-157, Oeiras, Portugal*

² *Research Unit Biopolymers Interaction Assemblies, INRAE, 44316 Nantes, France*

* *corresponding author: Cristina Silva Pereira*

(spereira@itqb.unl.pt)

Supporting Information contains 27 pages including 35 Figures and 5 Tables.

Index of supplemental Tables and Figures (by order of appearance in the manuscript)

- **Figure S1-** ¹H spectral characterization of POM^{I-II} and POM^{III-IV}
- **Figure S2-** 2D-¹H-¹H COSY-NMR spectrum (CORrelated SpectroscopY) from POM^{I-II}.
- **Figure S3-** 2D-¹H-¹³C HSQC-NMR spectrum (Heteronuclear Single Quantum Coherence) from POM^{I-II}.
- **Figure S4-** 2D-¹H-¹³C HMBC-NMR spectrum (Heteronuclear Multiple Bond Coherence) from POM^{I-II}.
- **Figure S6-** 2D-¹H-¹³C HSQC-NMR spectrum (Heteronuclear Single Quantum Coherence) from POM^{III-IV}.
- **Figure S7-** 2D-¹H-¹³C HMBC-NMR spectrum (Heteronuclear Multiple Bond Coherence) from POM^{III-IV}.
- **Figure S8-** 2D-¹H-¹³C HSQC (Heteronuclear Single Quantum Coherence) -NMR spectra of French pomace and its minor constituents: Peels (A3.3), Seeds (A4.3) and Fibers (A5.3) in the aromatics region. Some assignments (unlabelled) are uncertain or unidentified.
- **Figure S9-** (A) Principal Component Analysis (PC1;PC2) and the PCA loadings of the monomeric compounds of cutin from POM^{III-IV} and cutin from POM^{I-II} and (B) the ANOVA pair wise statistical analysis between the monomeric composition of each cutin ($p > 0.05$).
- **Figure S10-** 2D-¹H-¹³C HSQC (Heteronuclear Single Quantum Coherence) spectral characterization of POM^{I-II} and POM^{III-IV} and each cutin-rich material overlap.
- **Table S1** - Quantitative Analyses of Total Carbohydrate Content in cutin-rich materials.
- **Figure S11-** ¹H NMR spectra of the alkaline hydrolysis fractions of cutin from POM^{I-II}. After 1 hour of hydrolysis using 1M NaOH the soluble fraction (COM1^S) and the precipitated fractions (COM1^P) were analysed by ¹H NMR.

- **Figure S12-** 2D ^1H - ^1H COSY-NMR spectrum (CORrelated SpectroscopY) of COM1^P after 1 hour of hydrolysis using 1M NaOH upon Cutin from POM^{I-II}.
- **Figure S13-** 2D- ^1H - ^{13}C HMBC-NMR spectrum (Heteronuclear Multiple Bond Coherence) of COM1^P after 1 hour of hydrolysis using 1M NaOH upon Cutin from POM^{I-II}.
- **Figure S14-** 2D- ^1H - ^1H COSY-NMR spectrum (CORrelated SpectroscopY) of COM1^S after 1 hour of hydrolysis using 1M NaOH upon Cutin from POM^{I-II}.
- **Figure S15-** 2D- ^1H - ^{13}C HMBC-NMR spectrum (Heteronuclear Multiple Bond Coherence) of COM1^S after 1 hour of hydrolysis using 1M NaOH upon Cutin from POM^{I-II}.
- **Figure S16-** ^1H NMR spectra of the methanolysis fractions of cutin from POM^{I-II}. After 2 hours of hydrolysis using 0.1M NaOCH₃ the soluble fraction (COM2^S) and the precipitated fractions (COM2^P) were analysed by ^1H NMR.
- **Figure S17-** 2D ^1H - ^1H COSY-NMR spectrum (CORrelated SpectroscopY) of COM2^P after 2 hours of hydrolysis using 0.1M NaOCH₃ upon Cutin from POM^{I-II}.
- **Figure S18-** 2D- ^1H - ^{13}C HMBC-NMR spectrum (Heteronuclear Multiple Bond Coherence) of COM2^P after 2 hours of hydrolysis using 0.1M NaOCH₃ upon Cutin from POM^{I-II}.
- **Figure S19-** 2D- ^1H - ^1H COSY-NMR spectrum (CORrelated SpectroscopY) of COM2^S after 2 hours of hydrolysis using 0.1M NaOCH₃ upon Cutin from POM^{I-II}.
- **Figure S20-** 2D- ^1H - ^{13}C HMBC-NMR spectrum (Heteronuclear Multiple Bond Coherence) of COM2^S after 2 hours of hydrolysis using 0.1M NaOCH₃ upon Cutin from POM^{I-II}.
- **Figure S21-** ^1H NMR spectra of the alkaline hydrolysis fractions of cutin from POM^{III-IV}. After 1 hour of hydrolysis using 1M NaOH the soluble fraction (COM3^S) and the precipitated fractions (COM3^P) were analysed by ^1H NMR.
- **Figure S22-** 2D ^1H - ^1H COSY-NMR spectrum (CORrelated SpectroscopY) and 2D- ^1H - ^{13}C HMBC-NMR spectrum (Heteronuclear Multiple Bond Coherence) of COM3^P after 1 hour of hydrolysis using 1M NaOH upon Cutin from POM^{III-IV}.
- **Figure S23-** 2D- ^1H - ^1H COSY-NMR spectrum (CORrelated SpectroscopY) of COM3^S after 1 hour of hydrolysis using 1M NaOH upon Cutin from POM^{III-IV}.
- **Figure S24-** 2D- ^1H - ^{13}C HMBC-NMR spectrum (Heteronuclear Multiple Bond Coherence) of COM3^S after 1 hour of hydrolysis using 1M NaOH upon Cutin from POM^{III-IV}.
- **Figure S25-** ^1H NMR spectra of the methanolysis fractions of cutin from POM^{III-IV}. After 2 hours of hydrolysis using 0.1M NaOCH₃ the soluble fraction (COM4^S) and the precipitated fractions (COM4^P) were analysed by ^1H NMR.
- **Figure S26-** 2D- ^1H - ^1H COSY-NMR spectrum (CORrelated SpectroscopY) of COM4^P after 2 hours of hydrolysis using 0.1M NaOCH₃ upon Cutin from POM^{III-IV}.
- **Figure S27-** 2D- ^1H - ^{13}C HMBC-NMR spectrum (Heteronuclear Multiple Bond Coherence) of COM4^P after 2 hours of hydrolysis using 0.1M NaOCH₃ upon Cutin from POM^{III-IV}.

- **Figure S28-** 2D-¹H-¹H COSY-NMR spectrum (CORrelated SpectroscopY) of COM4^S after 2 hours of hydrolysis using 0.1M NaOCH₃ upon Cutin from POM^{III-IV}.
- **Figure S29-** 2D-¹H-¹³C HMBC-NMR spectrum (Heteronuclear Multiple Bond Coherence) of COM4^S after 2 hours of hydrolysis using 0.1M NaOCH₃ upon Cutin from POM^{III-IV}.
- **Figure S30-** ³¹P NMR spectra of COMs. The regions highlighted were used to quantify the OH-aliphatics, OH-aromatics and OH-free acids.
- **Figure S31-** 2D-¹H-¹³C - HSQC spectral characterization peels (A,B,C) and seed's (D,E,F) hydrolysates in aliphatics (A,D) glycerol CH-Acyl (B,E) and aromatics (C,F) region. Blue color stands for the soluble fraction and red color stands for the precipitated fraction. Some assignments (unlabelled) are uncertain or unidentified.
- **Figure S32-** Principal Component Analysis (PC1;PC2) and the PCA loadings of the NMR features of COM's
- **Figure S33-** Antimicrobial activity comparing an oligomeric fraction with ethyl esters (COM2^P) and one without ethyl esters (COM2^PØ) in both *S.aureus* (A) and *E.coli* (B) . Pairwise t-tests comparisons were used to identify significant differences between COM samples (p <0.05) and the results showed no statistical difference between the samples (n.s P > 0.05). (C) GC-MS quantitative analysis of monomeric constituents of COM2^P and COM2^P Ø.
- **Table S2 -** Quantitative analysis of the constituents of COM's by GC-MS. Results are given as mg of compound per g of starting material. The identification yields are indicated below and represent the ratio between the identified peak area and the total area of peaks in the chromatogram. Monomers that were not detected in a specific sample are labelled as n.d.
- **Table S3 -** Quantitative analysis of the constituents of COM's by GC-MS. Results are given as mg of compound per g of starting material. The identification yields are indicated below and represent the ratio between the identified peak area and the total area of peaks in the chromatogram. Monomers that were not detected in a specific sample are labelled as n.d.
- **Figure S34-** Principal Component Analysis (PC1; PC3) and the PCA loadings of the GC-MS data of the hydrolysable monomers identified in the COMs.
- **Table S4-** Reported minimal inhibitory concentration (MIC)¹⁻⁵ of cutin monomers for *S. aureus* and *E. coli* and the concentration (mM) of monomers in each COM sample at 1000ug/mL, as determined by GC-MS.
- **Figure S35-** Heatmap of the ratios of monomers (hydrolysed /non-hydrolysed) present in each COM. Scaled from 0 to 5; values higher than 1 means that the monomer was linked in an oligomeric structure.
- **Table S5-** Recovery yield (%) of cutin-rich materials from pomace and production yields (%) of each COM fraction. Mean values obtained from 3 replicates and the respective standard deviation (SD) are shown.

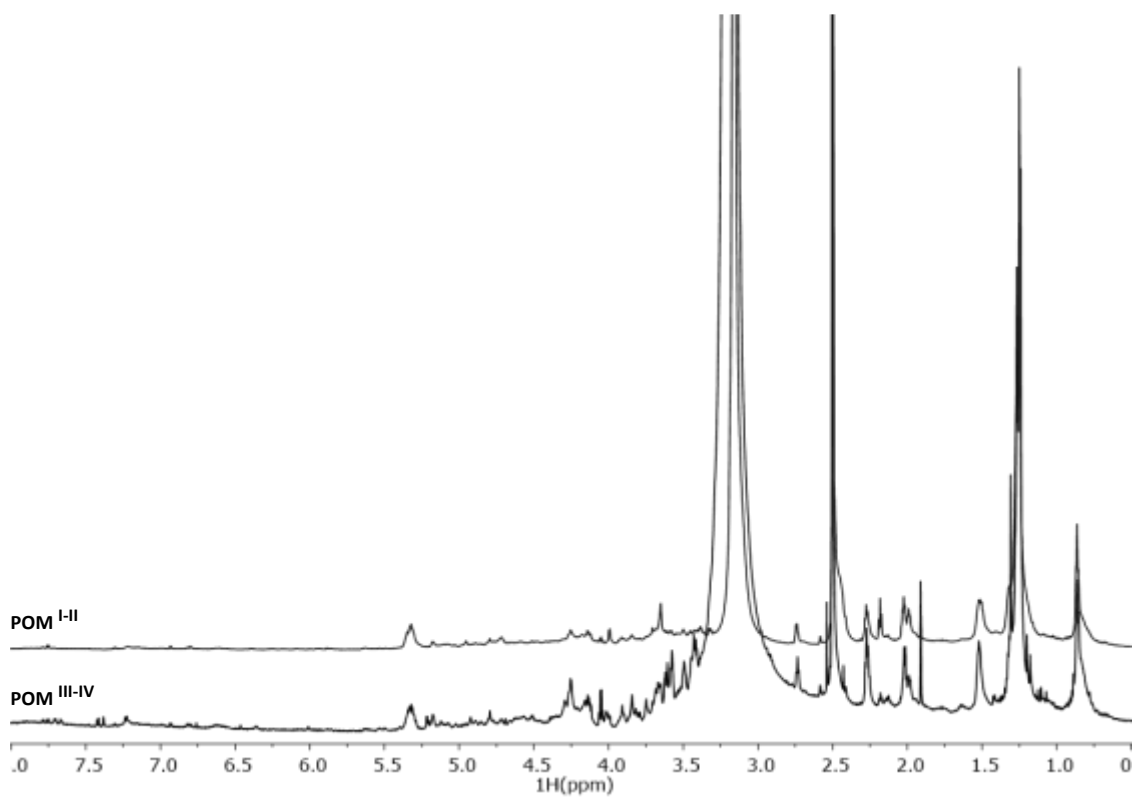


Figure S1- ^1H spectral characterization of $\text{POM}^{\text{I-II}}$ and $\text{POM}^{\text{III-IV}}$.

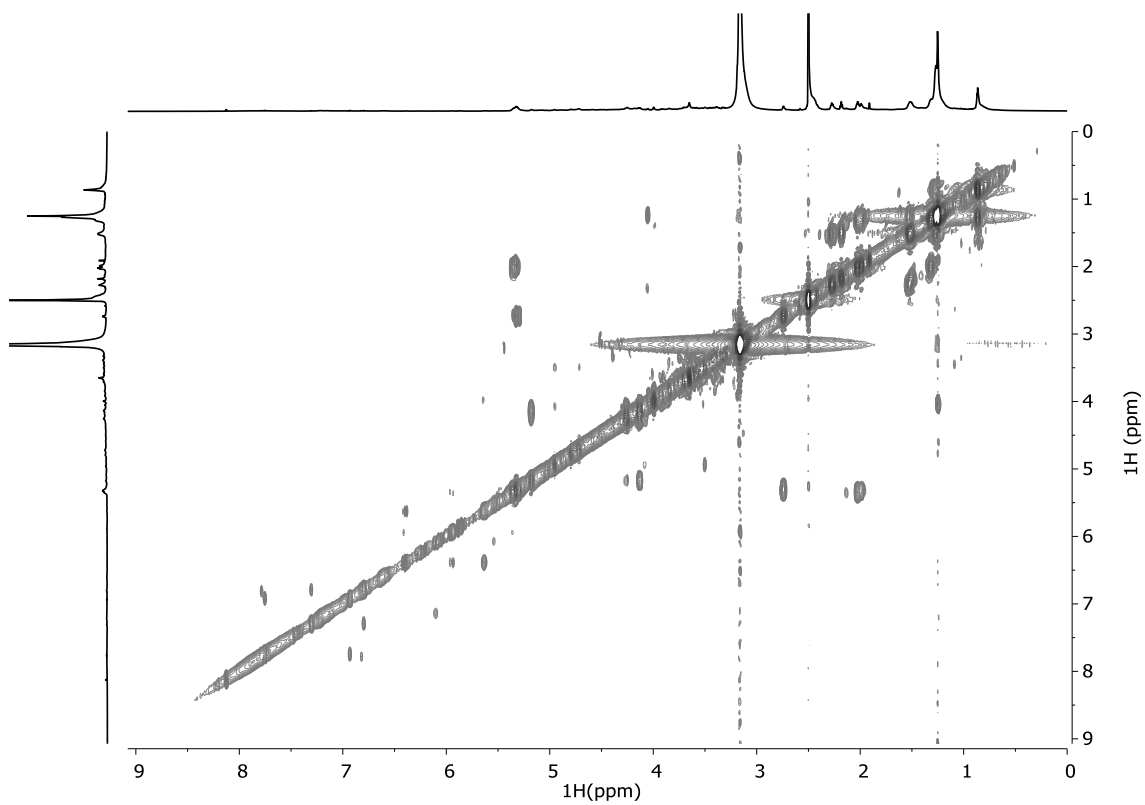


Figure S2- 2D- ^1H - ^1H COSY-NMR spectrum (COrrrelated SpectroscopY) from POM^{II}.

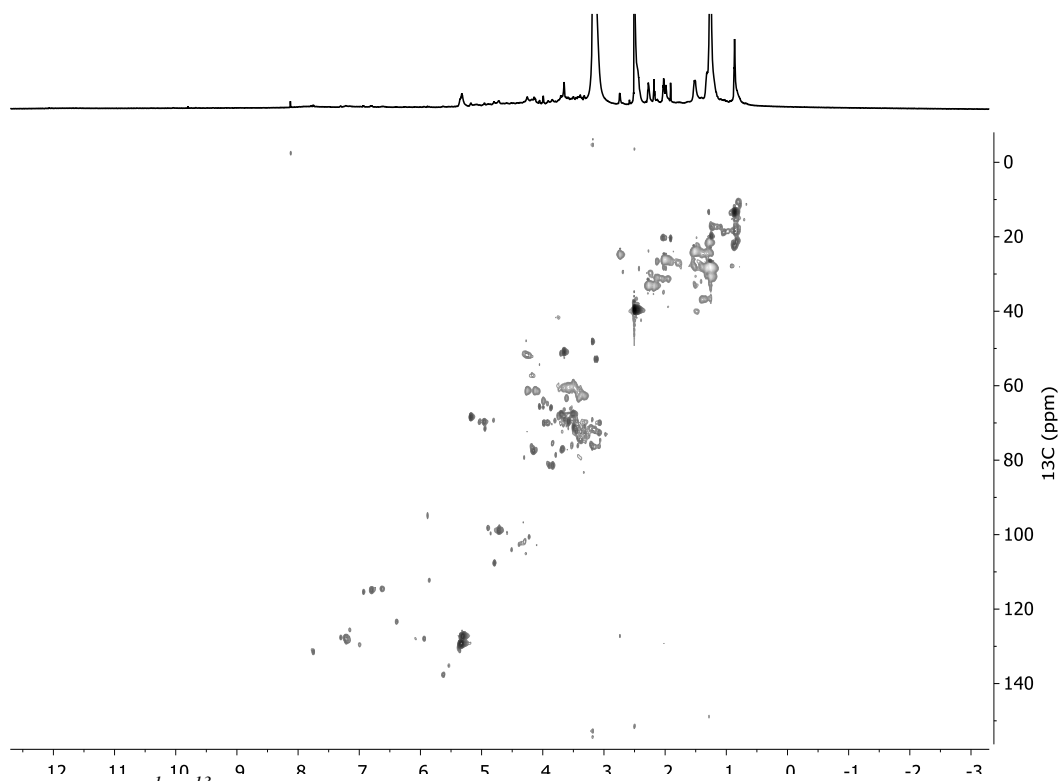


Figure S3- 2D- ^1H - ^{13}C HSQC-NMR spectrum (Heteronuclear Single Quantum Coherence) from POM^{II}.

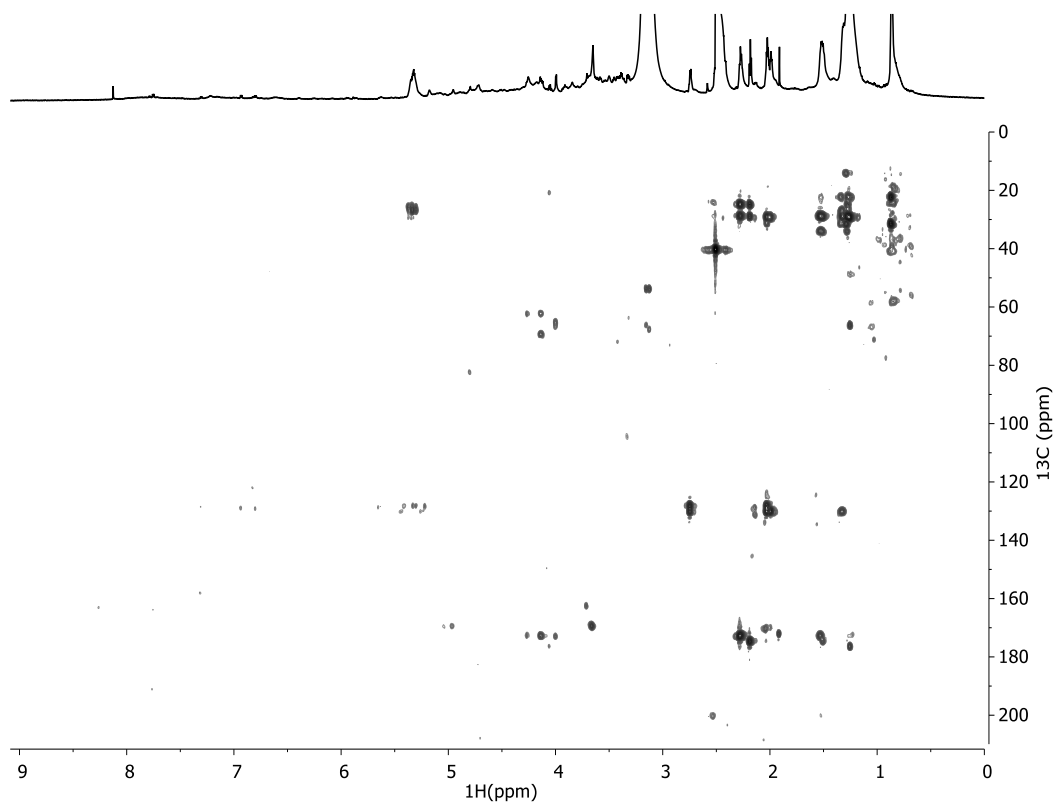


Figure S4- 2D- ^1H - ^{13}C HMBC-NMR spectrum (Heteronuclear Multiple Bond Coherence) from POM^{I-II}.

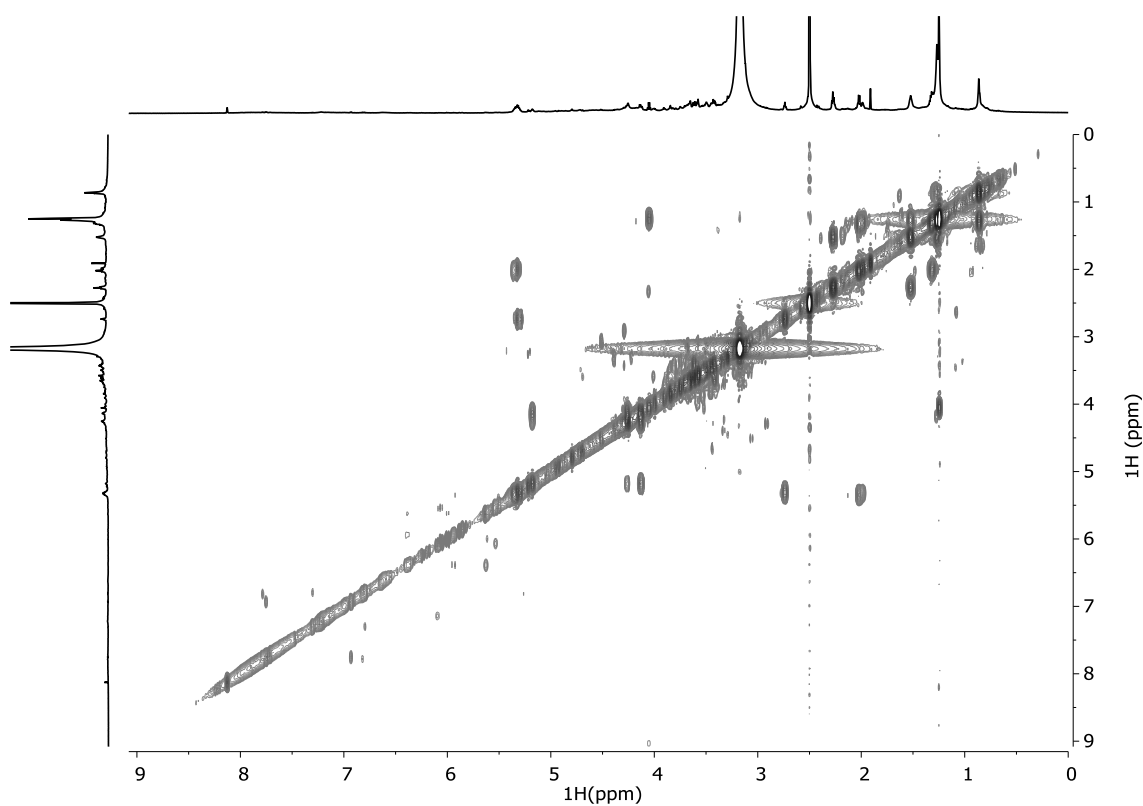


Figure S5- 2D- ^1H - ^1H COSY-NMR spectrum (CORrelated SpectroscopY) from POM^{III-IV}.

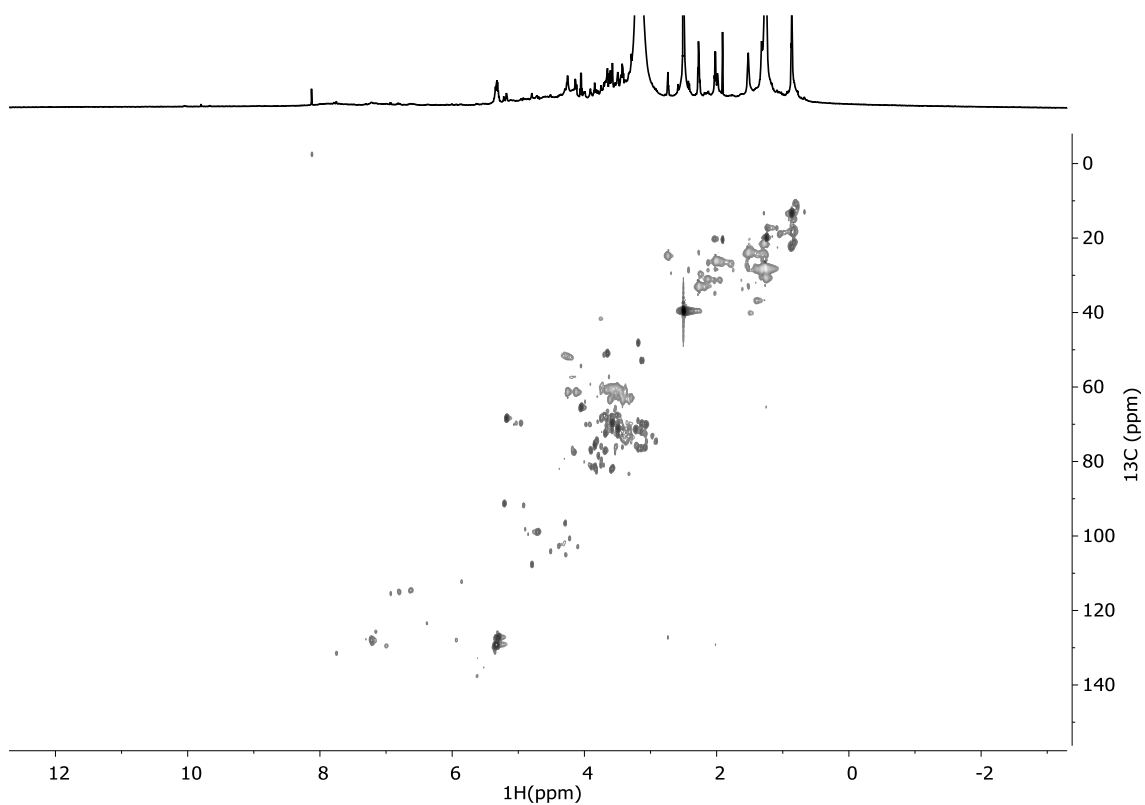


Figure S6- 2D- ^1H - ^{13}C HSQC-NMR spectrum (Heteronuclear Single Quantum Coherence) from $\text{POM}^{\text{III-IV}}$.

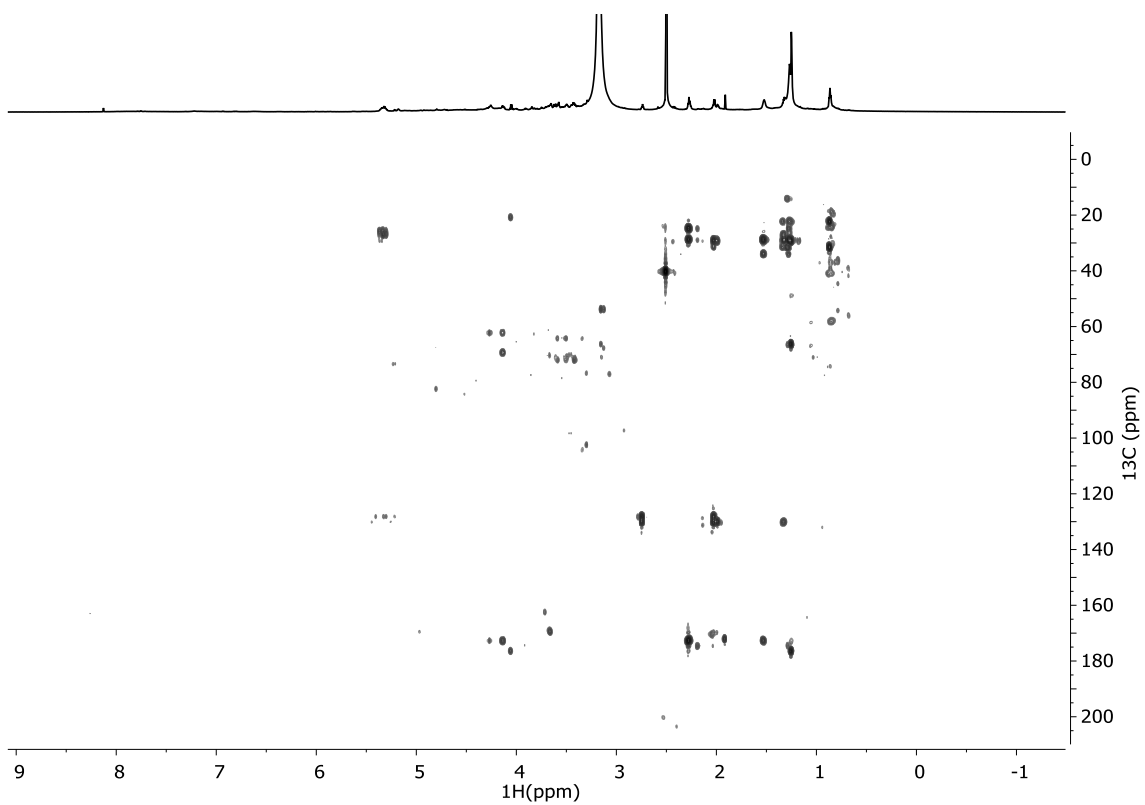


Figure S7- 2D- ^1H - ^{13}C HMBC-NMR spectrum (Heteronuclear Multiple Bond Coherence) from $\text{POM}^{\text{III-IV}}$.

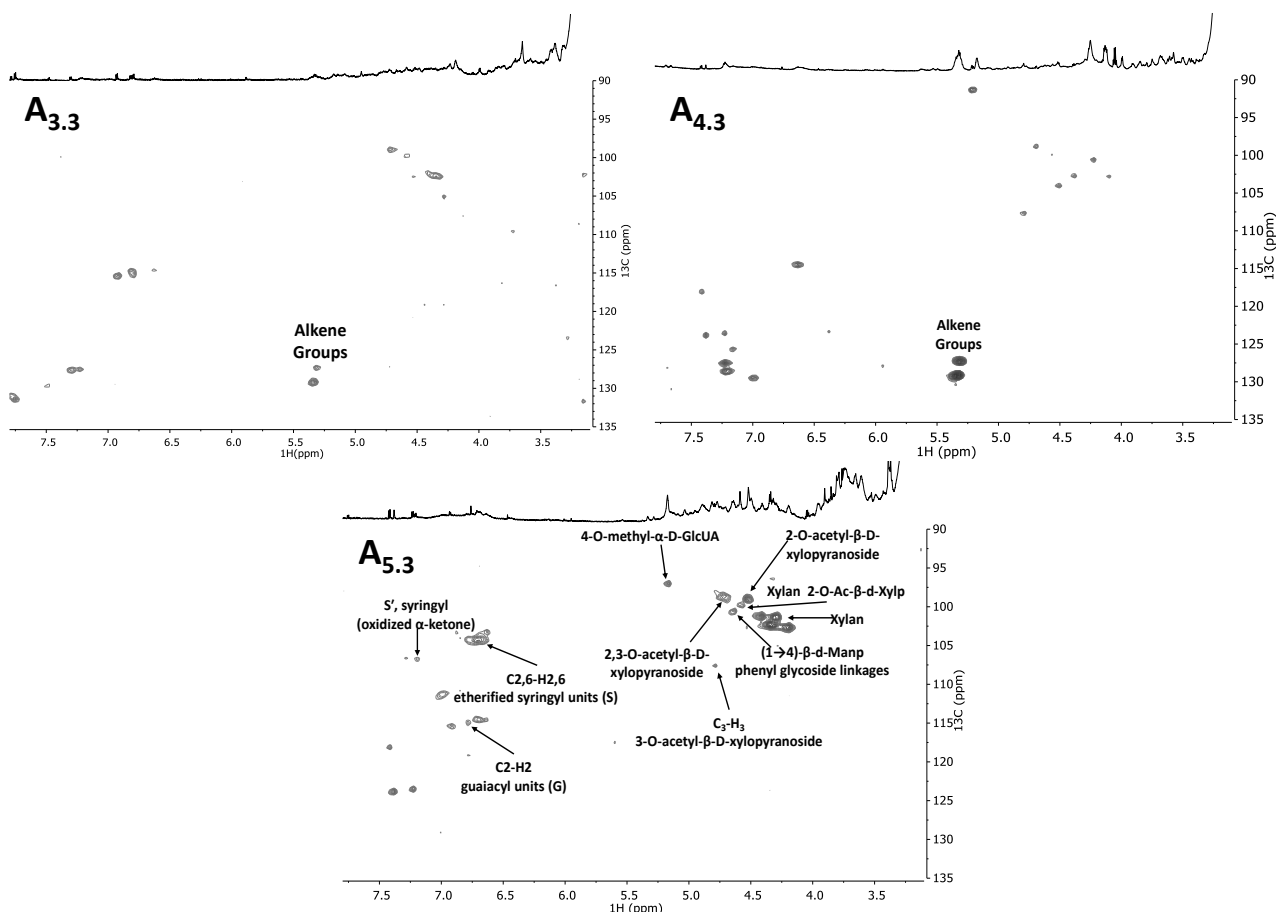


Figure S8- 2D-¹H-¹³C HSQC (Heteronuclear Single Quantum Coherence) -NMR spectra of French pomace and its minor constituents: Peels (A3.3), Seeds (A4.3) and Fibers (A5.3) in the aromatics' region. Some assignments (unlabeled) are uncertain or unidentified.

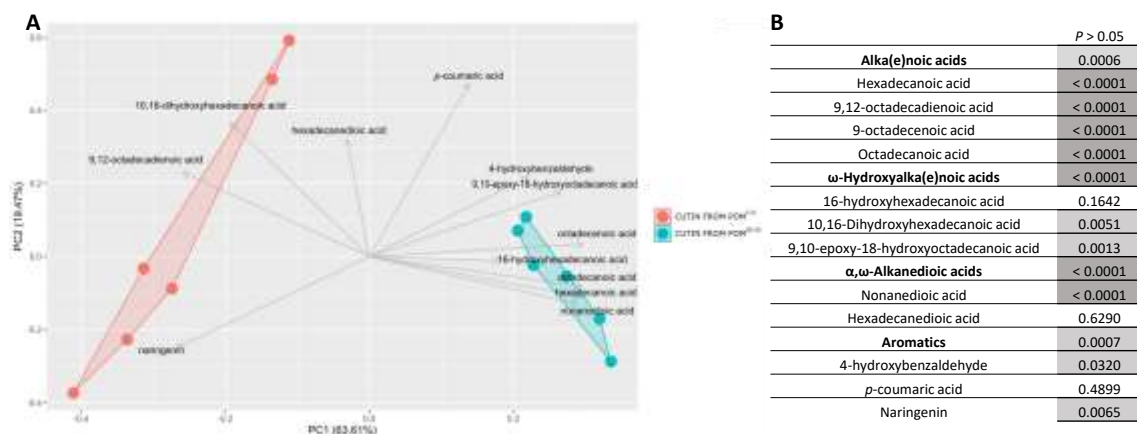


Figure S9- (A) Principal Component Analysis (PC1;PC2) and the PCA loadings of the monomeric compounds of cutin POM^{III-VI} and cutin from POM^{I-II} and (B) the ANOVA pair wise statistical analysis between the monomeric composition of each cutin (*p* > 0.05).

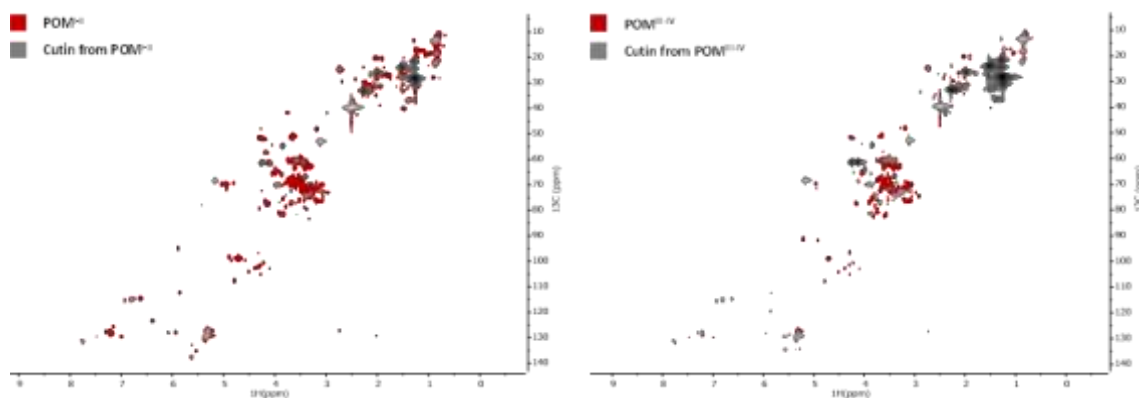


Figure S10- $2D-^1H-^{13}C$ HSQC (Heteronuclear Single Quantum Coherence) spectral characterization of POM^{I-II} and POM^{III-IV} and each cutin-rich material overlap.

Table S1- Quantitative Analyses of Total Carbohydrate Content in cutin-rich materials.

Cutin-rich material from:	ng (carbohydrate)/mg (sample)	carbohydrate content / %
POM^{I-II}	1.41 ± 0.29	$1.41E^{-4} \pm 2.93E^{-5}$
POM^{III-IV}	1.59 ± 0.14	$1.59E^{-4} \pm 1.36E^{-5}$

Quantitative Analyses of Total Carbohydrate Content. Samples were subjected to acid hydrolysis (1 M H_2SO_4 in methanol) for 4h at 90 °C. The hydrolysable sugars were recovered in the supernatant through centrifugation (18514 g, 4 °C, 20 min), and the pH was neutralized using 5 M NaOH in water. All samples were dried under a flux of nitrogen at room temperature. Quantification of carbohydrates in the dried hydrolysates was performed using the total carbohydrate assay kit from Sigma-Aldrich according to the manufacturer's instructions. The samples were analyzed in triplicate in two independent experiments.

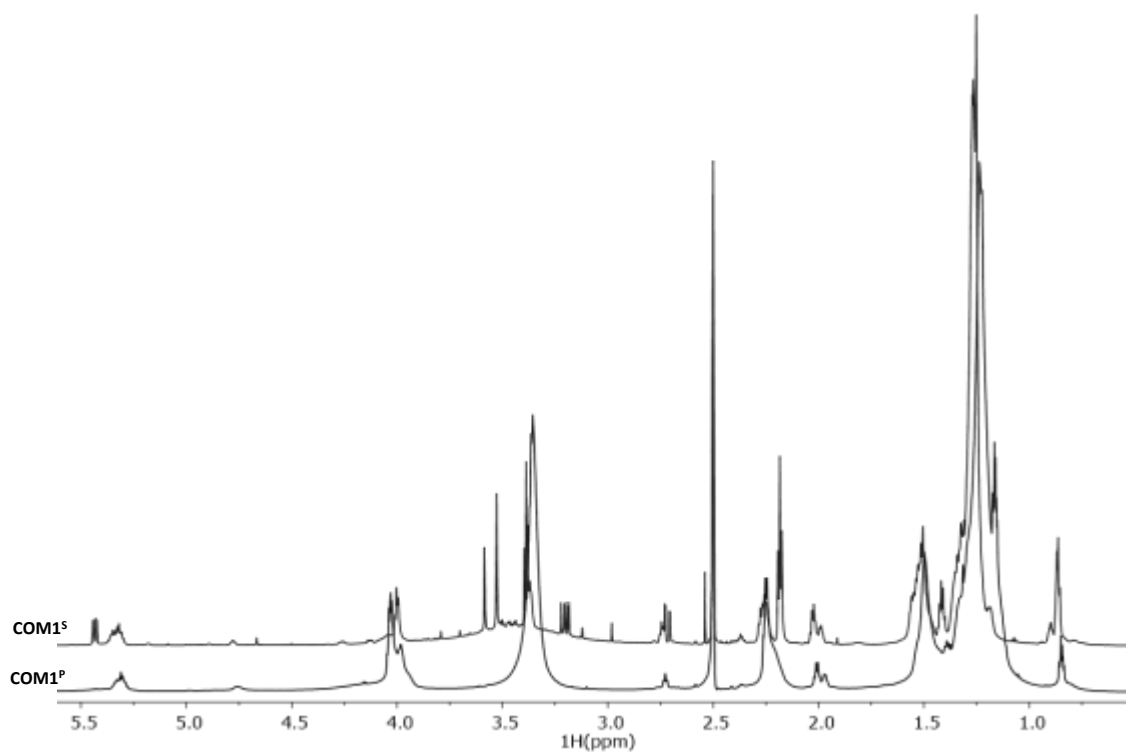


Figure S11- ^1H NMR spectra of the alkaline hydrolysis fractions of cutin from $\text{POM}^{\text{I-II}}$. After 1 hour of hydrolysis using 1M NaOH the soluble fraction (COM1^{S}) and the precipitated fractions (COM1^{P}) were analyzed by ^1H NMR.

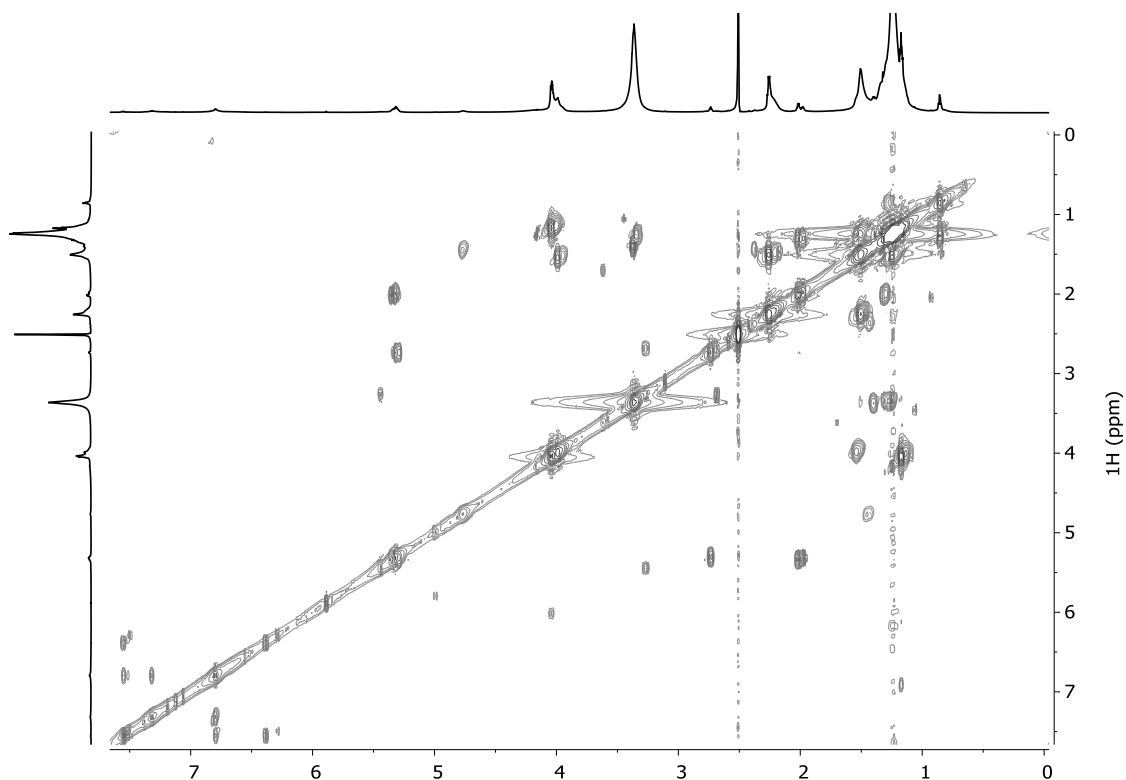


Figure S12- 2D ^1H - ^1H COSY-NMR spectrum (COrrelated Spectroscopy) of COM1^{P} after 1 hour of hydrolysis using 1M NaOH upon Cutin from $\text{POM}^{\text{I-II}}$.

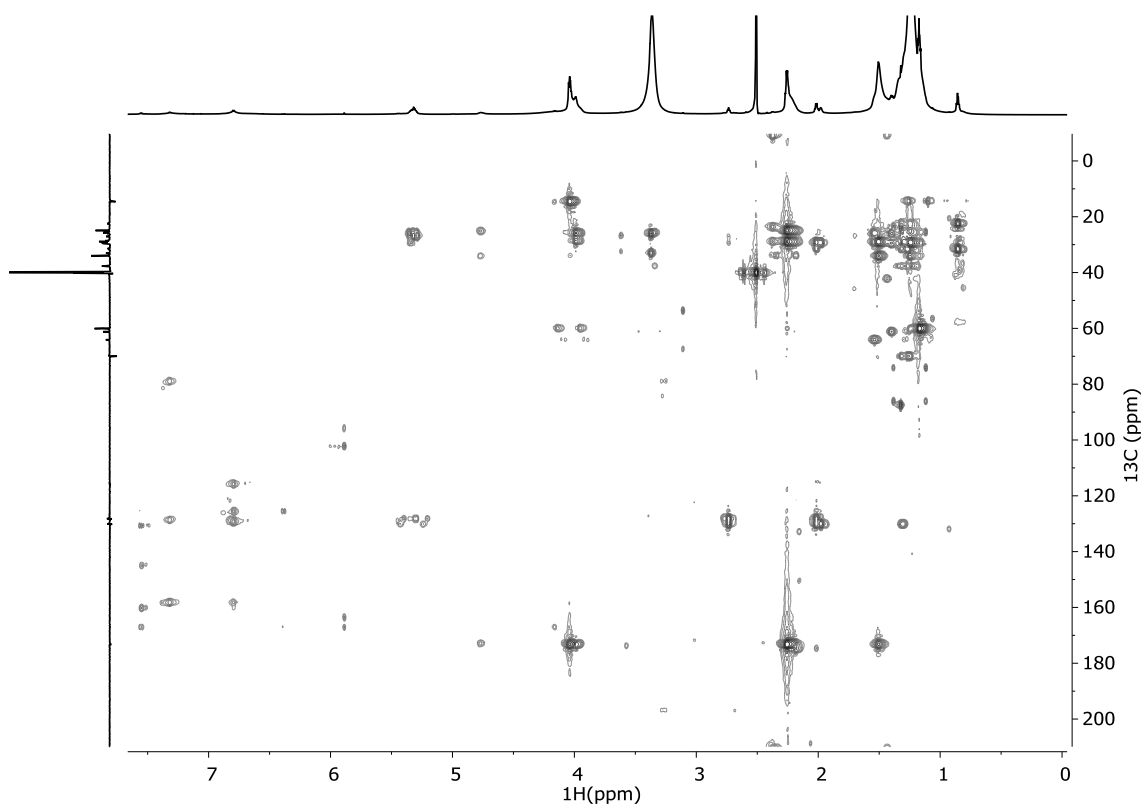


Figure S13- 2D ^1H - ^{13}C HMBC-NMR spectrum (Heteronuclear Multiple Bond Coherence) of COM1^P after 1 hour of hydrolysis using 1M NaOH upon Cutin from $\text{POM}^{\text{I-II}}$.

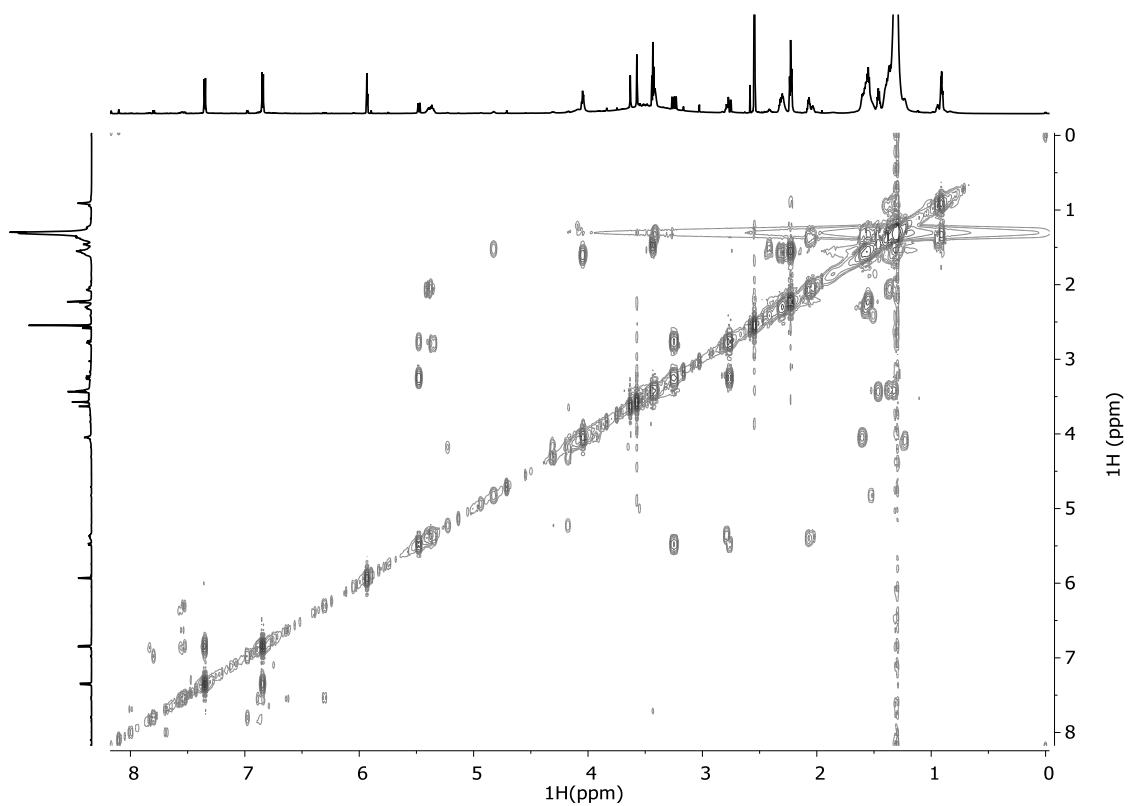


Figure S14- 2D ^1H - ^1H COSY-NMR spectrum (CORrelated SpectroscOPY) of COM1^S after 1 hour of hydrolysis using 1M NaOH upon Cutin from $\text{POM}^{\text{I-II}}$.

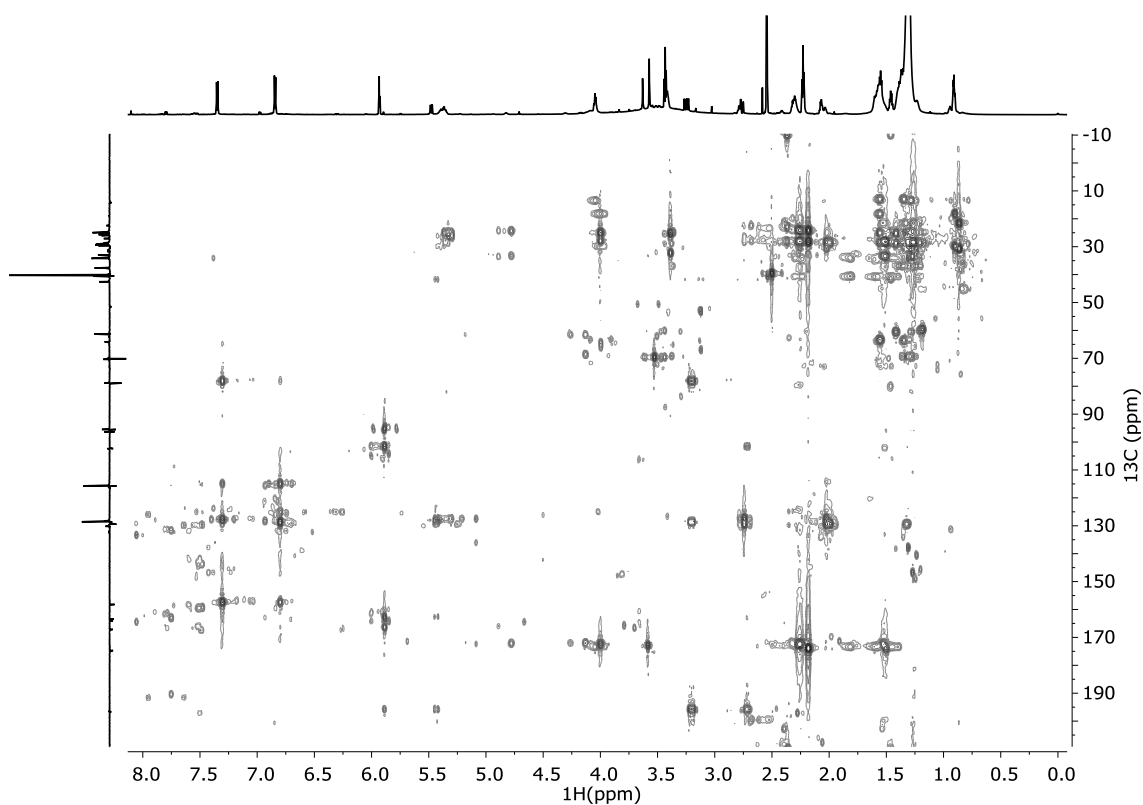


Figure S15- 2D- ^1H - ^{13}C HMBC-NMR spectrum (Heteronuclear Multiple Bond Coherence) of COM1^{S} after 1 hour of hydrolysis using 1M NaOH upon Cutin from $\text{POM}^{\text{I-II}}$.

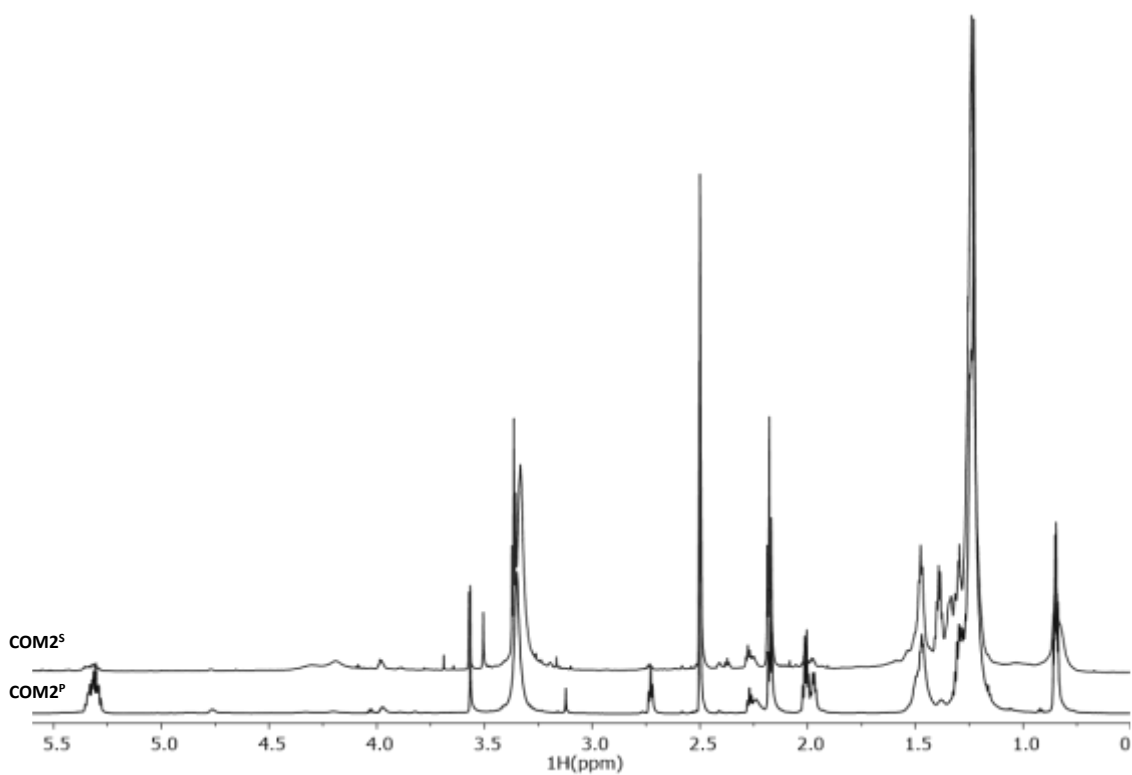


Figure S16- ^1H NMR spectra of the methanolysis fractions of cutin from $\text{POM}^{\text{I-II}}$. After 2 hours of hydrolysis using 0.1M NaOCH_3 the soluble fraction (COM2^{S}) and the precipitated fractions (COM2^{P}) were analyzed by ^1H NMR.

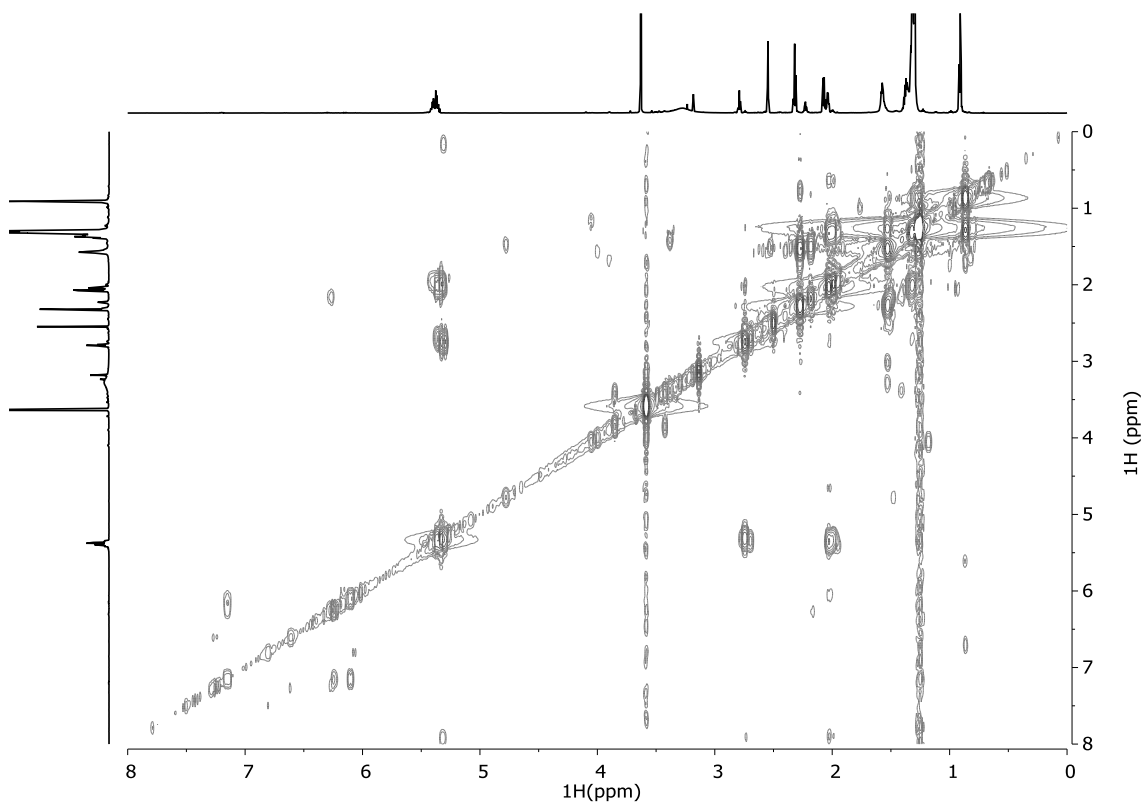


Figure S17- 2D $^{-1}\text{H}-^1\text{H}$ COSY-NMR spectrum (CORrelated SpectroscopY) of COM2^{P} after 2 hours of hydrolysis using 0.1M NaOCH_3 upon Cutin from $\text{POM}^{\text{I-II}}$.

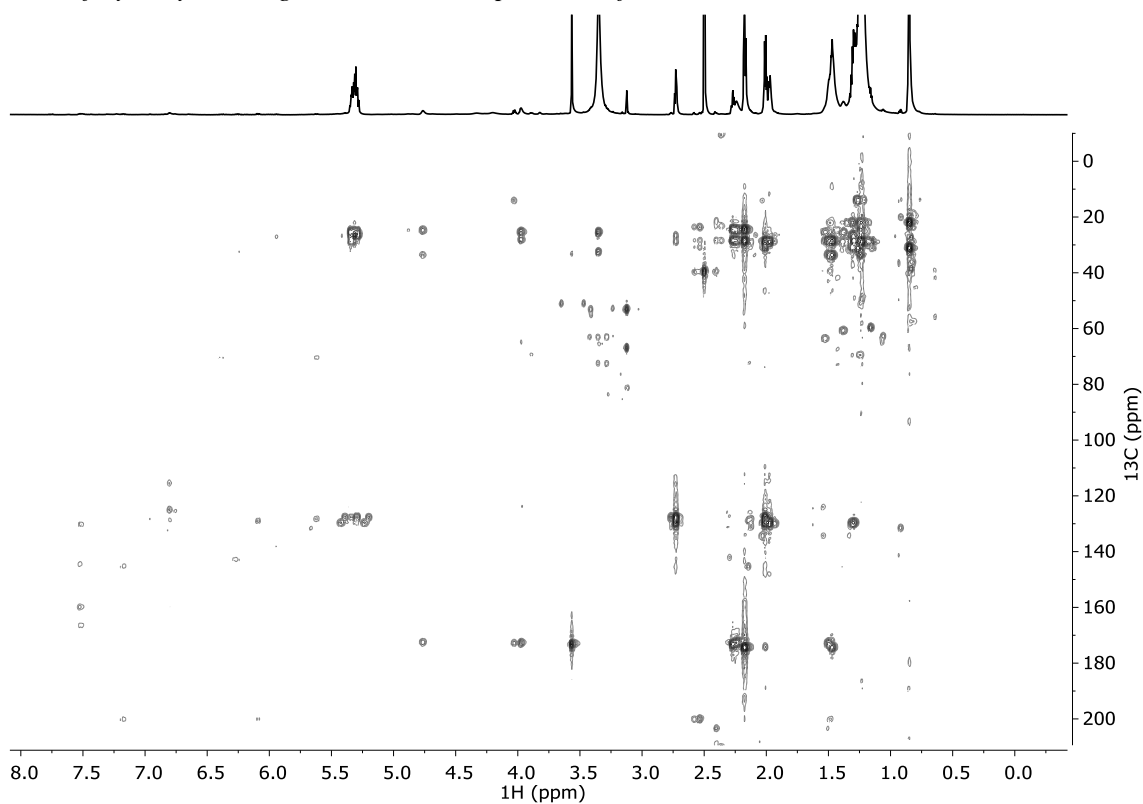


Figure S18- 2D $^{-1}\text{H}-^{13}\text{C}$ HMBC-NMR spectrum (Heteronuclear Multiple Bond Coherence) of COM2^{P} after 2 hours of hydrolysis using 0.1M NaOCH_3 upon Cutin from $\text{POM}^{\text{I-II}}$.

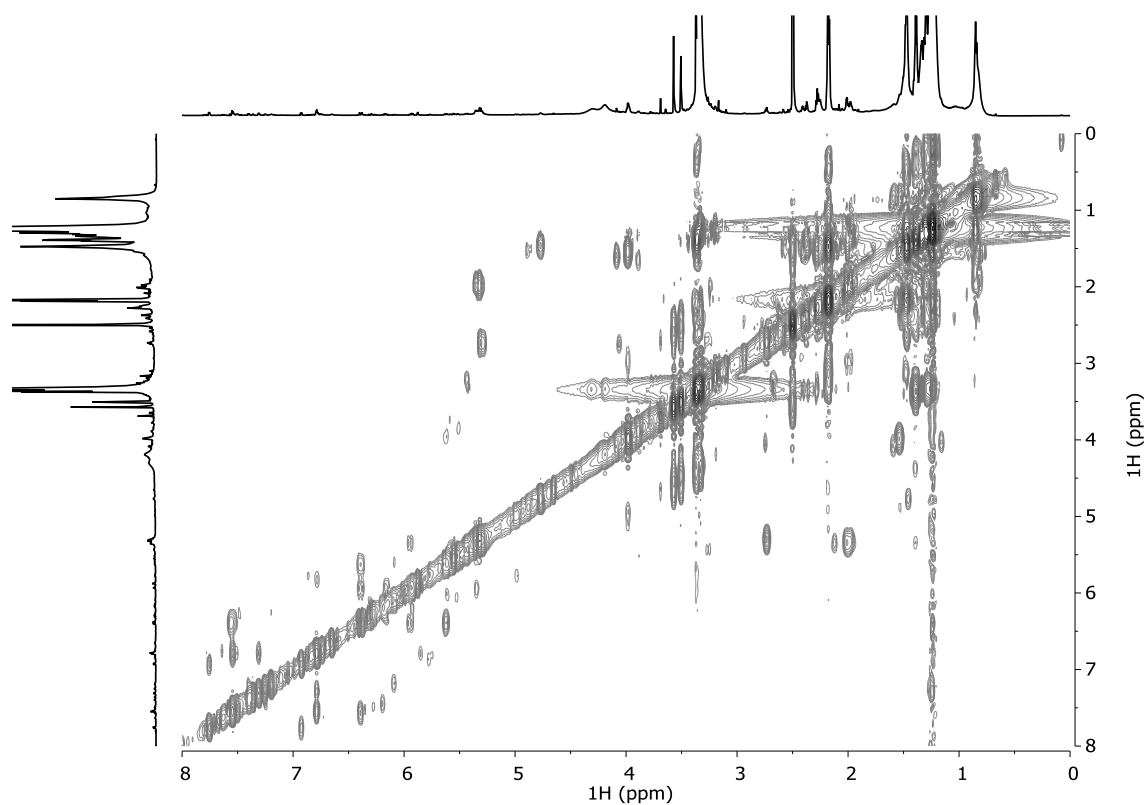


Figure S19- 2D ^1H - ^1H COSY-NMR spectrum (CORrelated SpectroscOPY) of COM2^{S} after 2 hours of hydrolysis using 0.1M NaOCH_3 upon Cutin from $\text{POM}^{\text{I-II}}$.

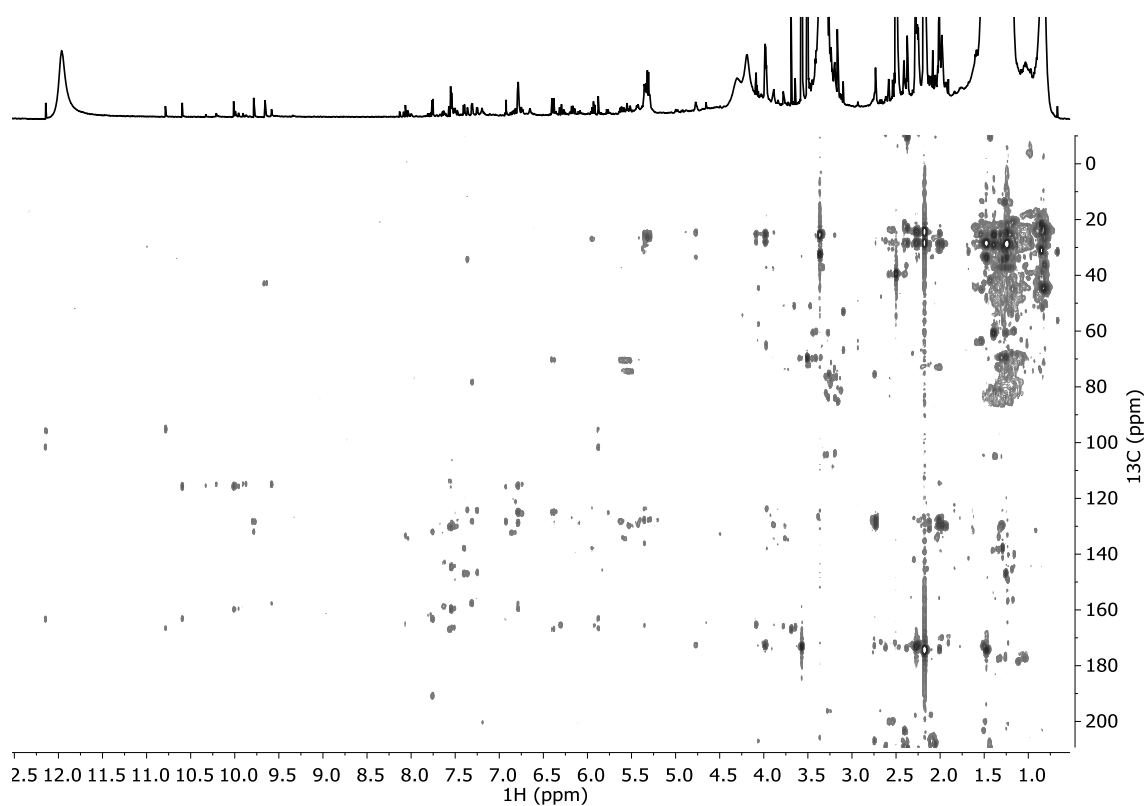


Figure S20- 2D ^1H - ^{13}C HMBC-NMR spectrum (Heteronuclear Multiple Bond Coherence) of COM2^{S} after 2 hours of hydrolysis using 0.1M NaOCH_3 upon Cutin from $\text{POM}^{\text{I-II}}$.

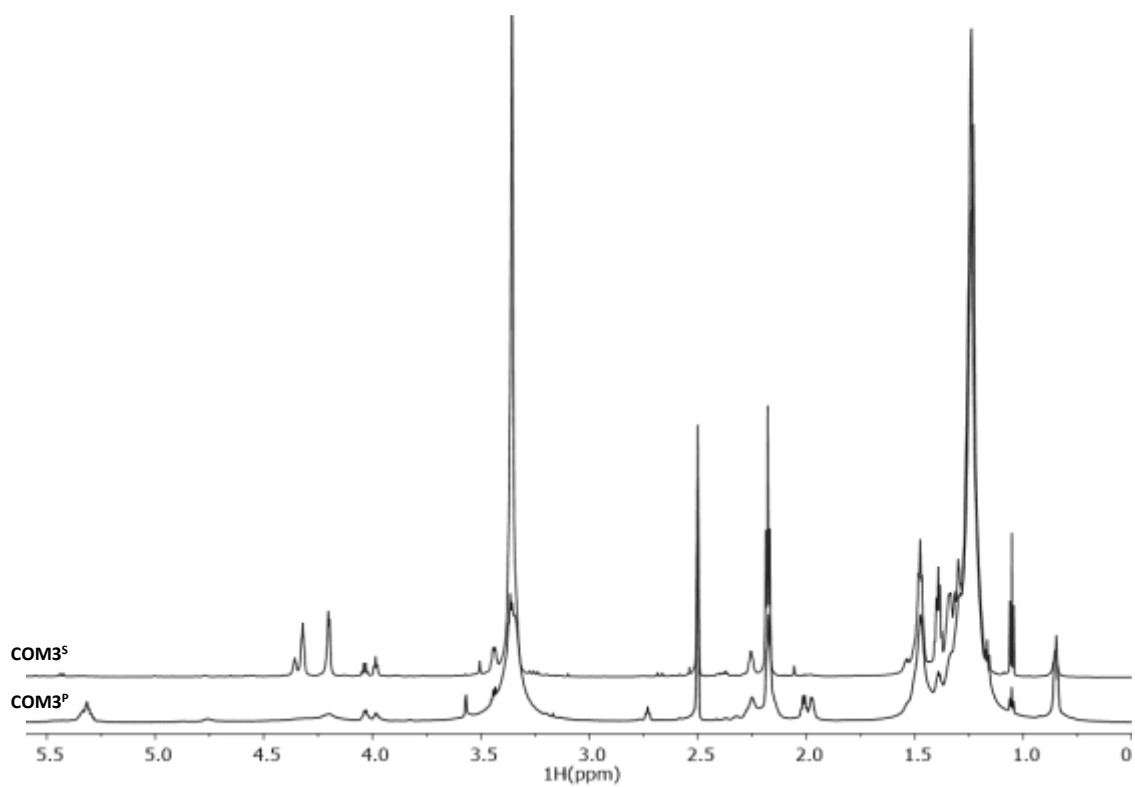


Figure S21- ¹H NMR spectra of the alkaline hydrolysis fractions of cutin from French pomace. After 1 hour of hydrolysis using 1M NaOH the soluble fraction (COM3^S) and the precipitated fractions (COM3^P) were analyzed by ¹H NMR.

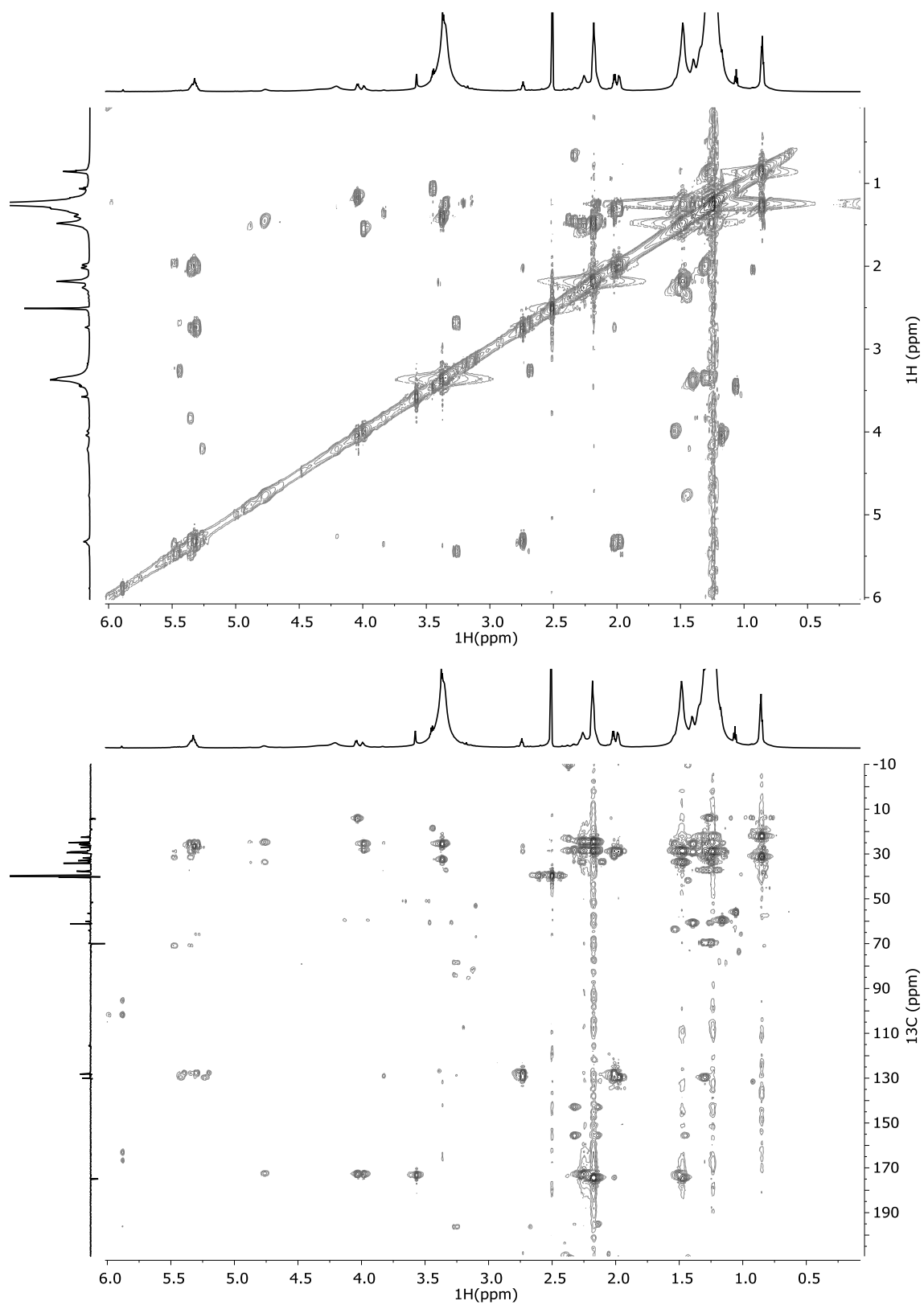


Figure S22- 2D ${}^1\text{H}$ - ${}^1\text{H}$ COSY-NMR spectrum (CORrelated SpectroscopY) and 2D ${}^1\text{H}$ - ${}^{13}\text{C}$ HMBNMR spectrum (Heteronuclear Multiple Bond Coherence) of COM3^P after 1 hour of hydrolysis using 1M NaOH upon Cutin from POM^{III-IV}.

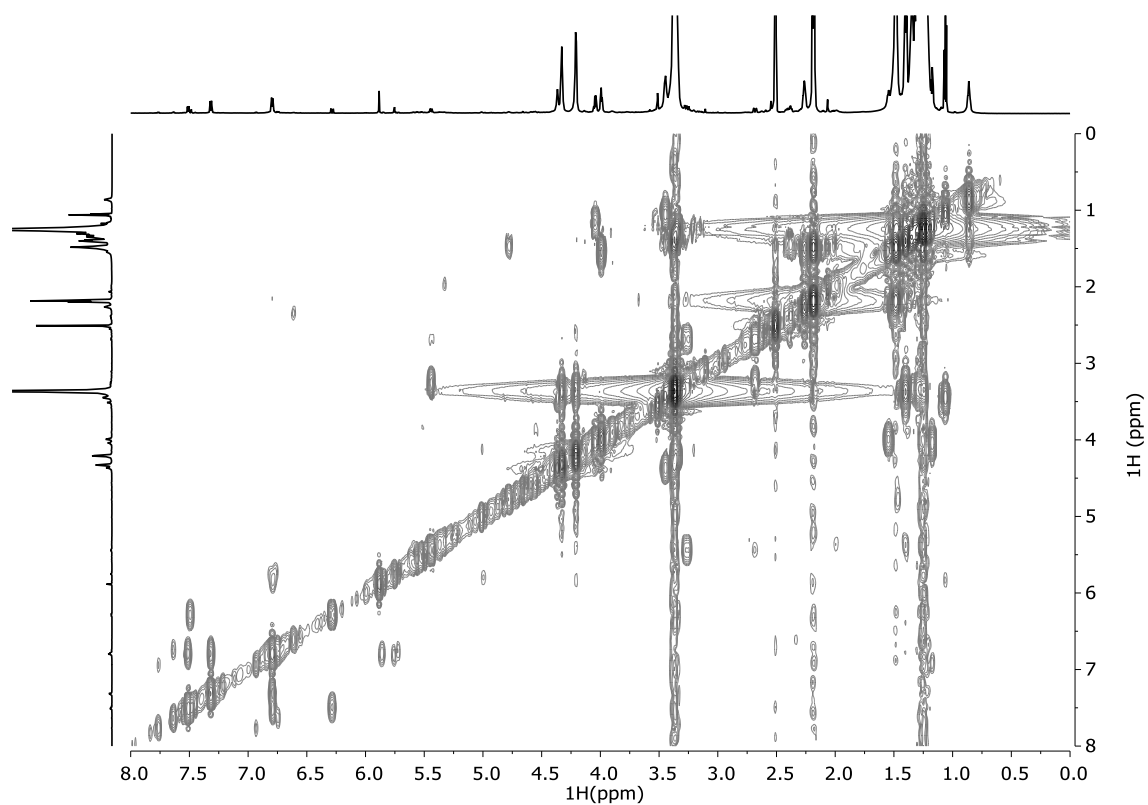


Figure S23- 2D ^1H - ^1H COSY-NMR spectrum (CORrelated SpectroscopY) of COM3^S after 1 hour of hydrolysis using 1M NaOH upon Cutin from POM^{III-IV}.

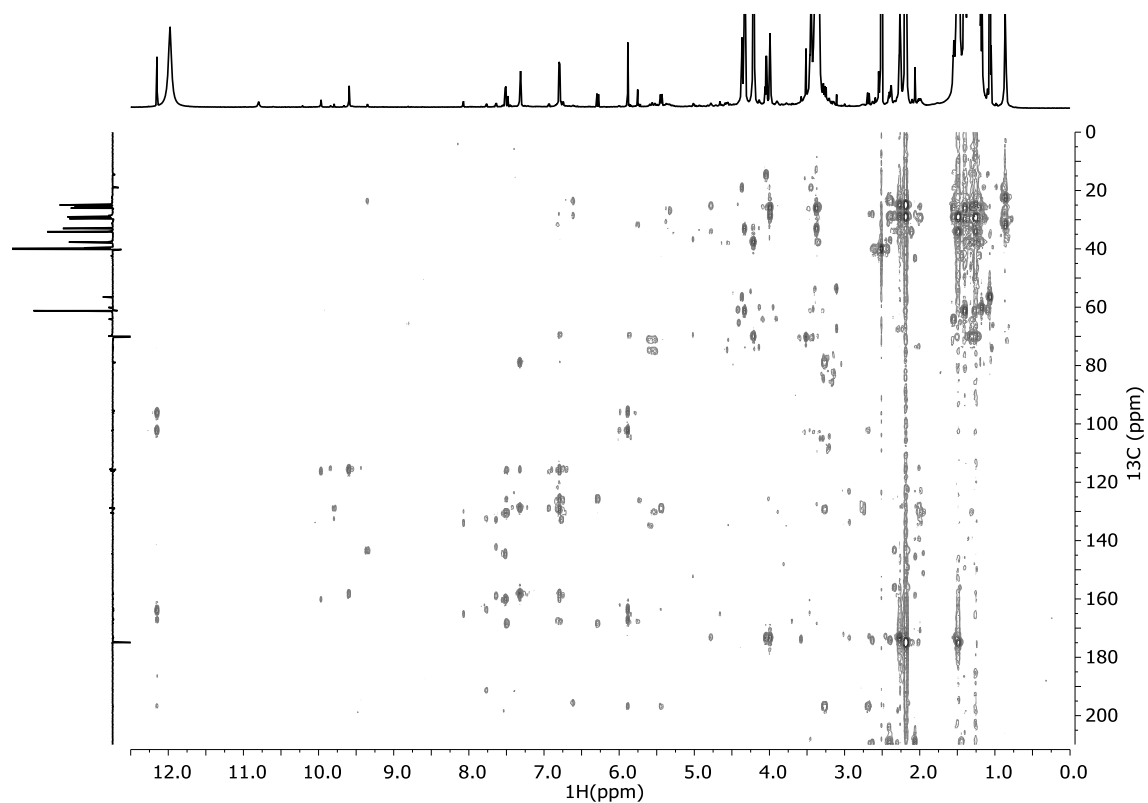


Figure S24- 2D ^1H - ^{13}C HMBC-NMR spectrum (Heteronuclear Multiple Bond Coherence) of COM3^S after 1 hour of hydrolysis using 1M NaOH upon Cutin from POM^{III-IV}.

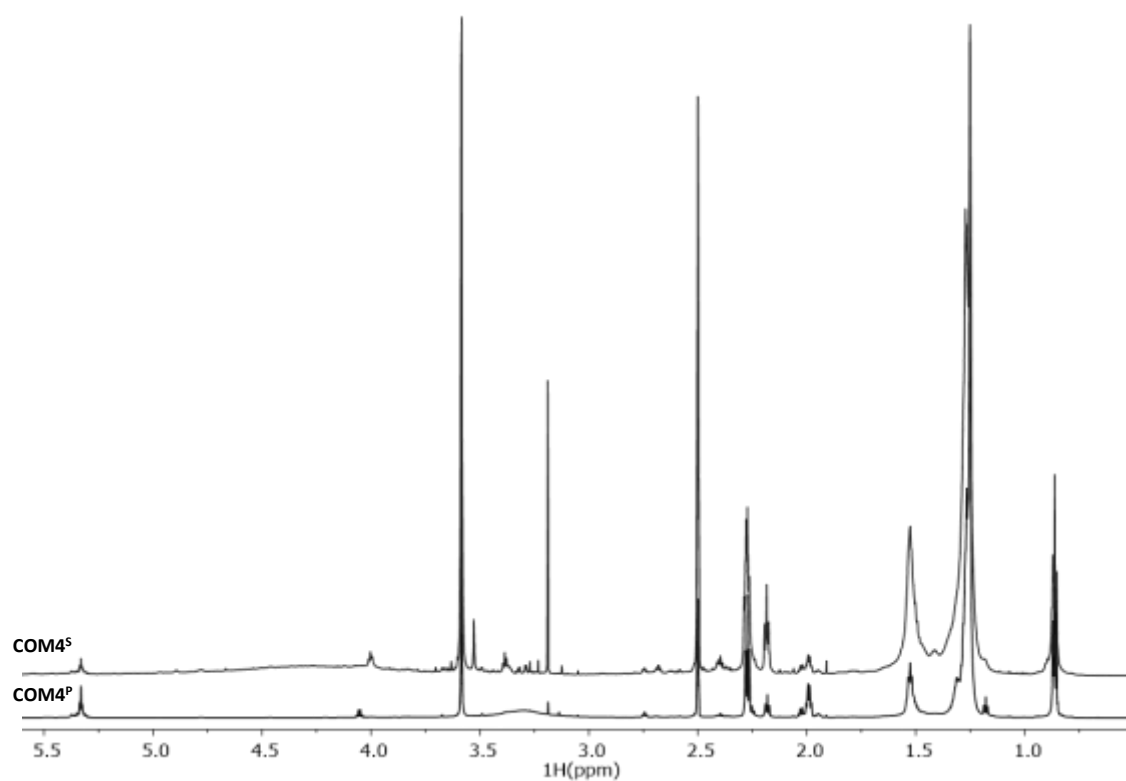


Figure S25- ^1H NMR spectra of the methanolysis fractions of cutin from French pomace. After 2 hours of hydrolysis using 0.1M NaOCH_3 the soluble fraction (COM4^{S}) and the precipitated fractions (COM4^{P}) were analyzed by ^1H NMR.

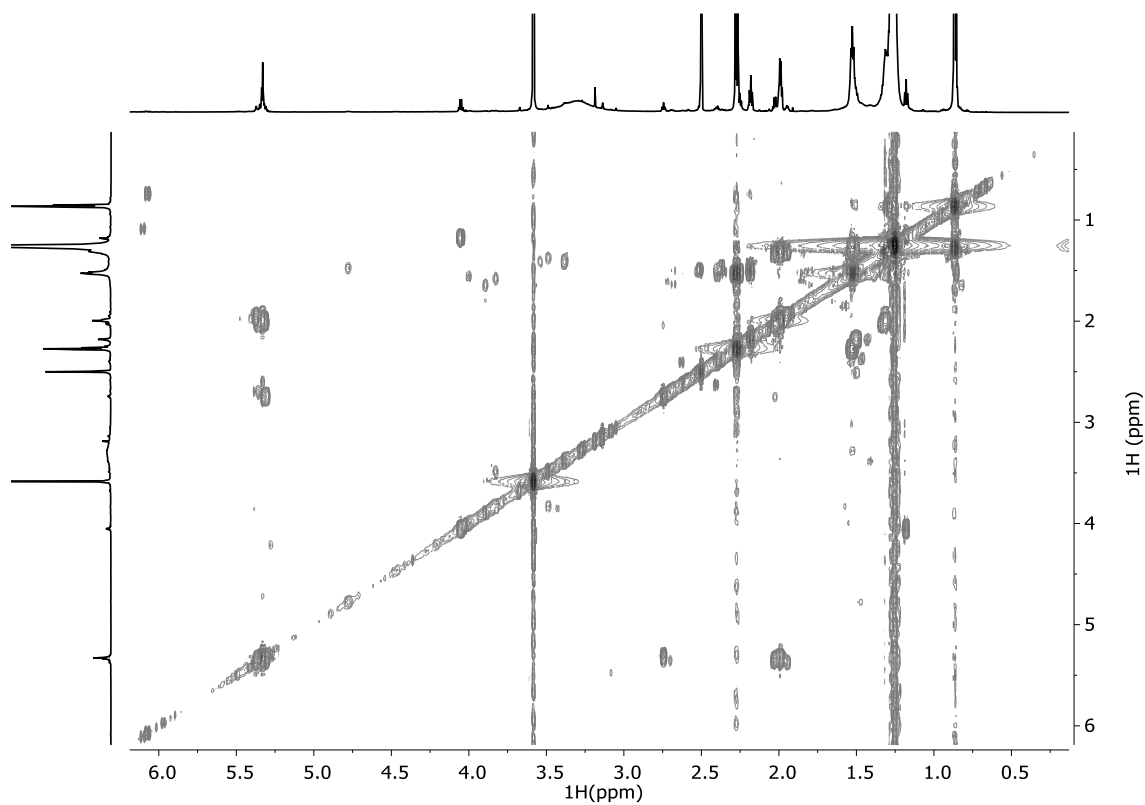


Figure S26- 2D ^1H - ^1H COSY-NMR spectrum (CORrelated SpectroscopY) of COM4P after 2 hours of hydrolysis using 0.1M NaOCH_3 upon Cutin from $\text{POM}^{\text{III-IV}}$.

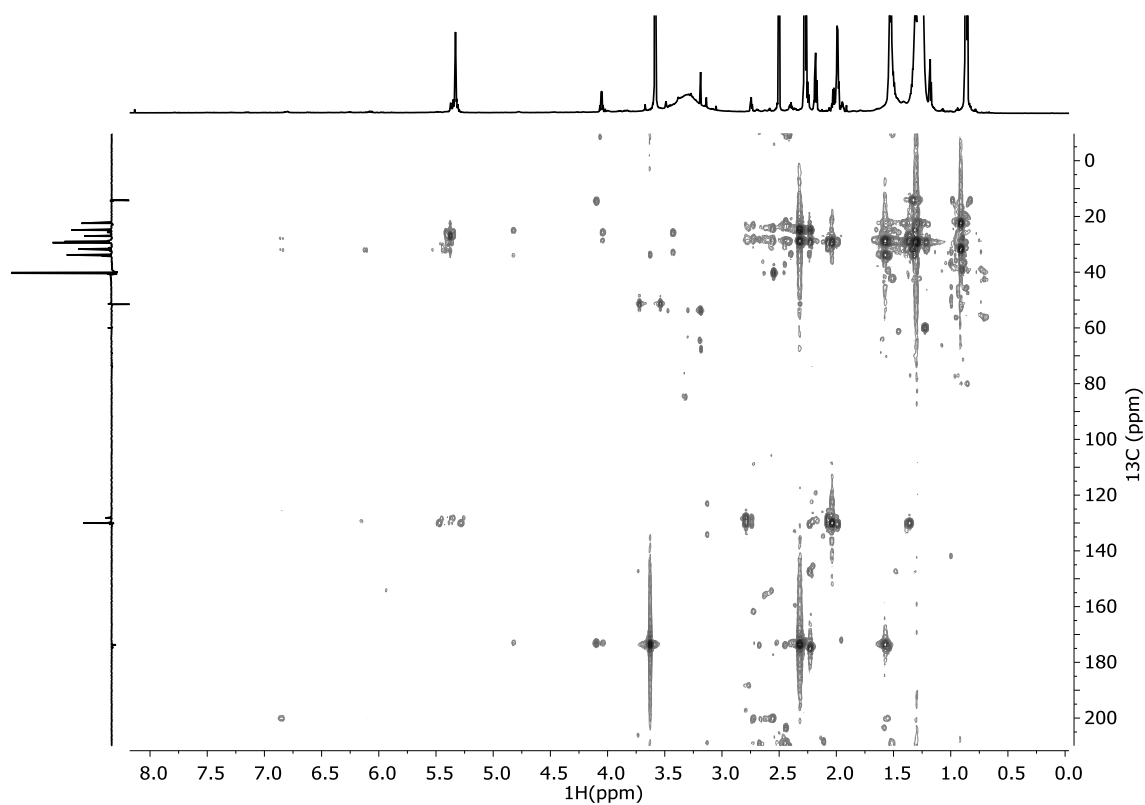


Figure S27- 2D - ^1H - ^{13}C HMBC-NMR spectrum (Heteronuclear Multiple Bond Coherence) of COM4^{P} after 2 hours of hydrolysis using 0.1M NaOCH_3 upon Cutin from $\text{POM}^{\text{III-IV}}$.

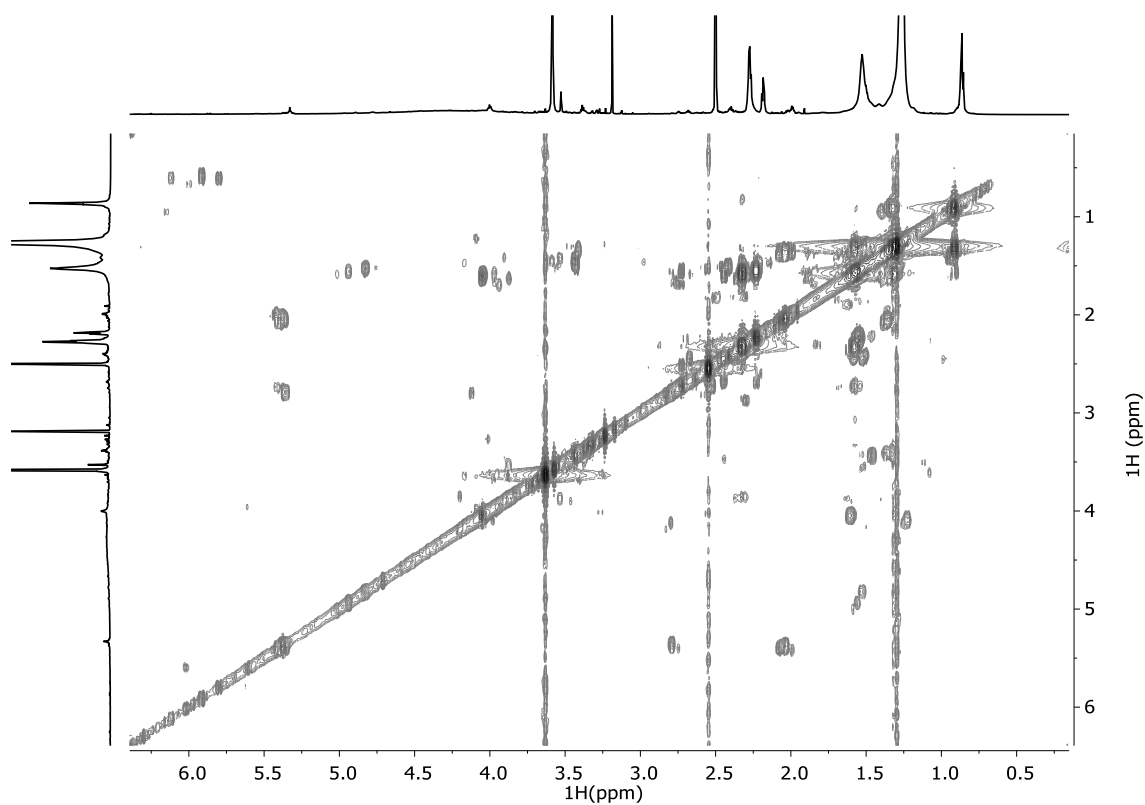


Figure S28- 2D - ^1H - ^1H COSY-NMR spectrum (CORrelated SpectroscOPY) of COM4^{S} after 2 hours of hydrolysis using 0.1M NaOCH_3 upon Cutin from $\text{POM}^{\text{III-IV}}$.

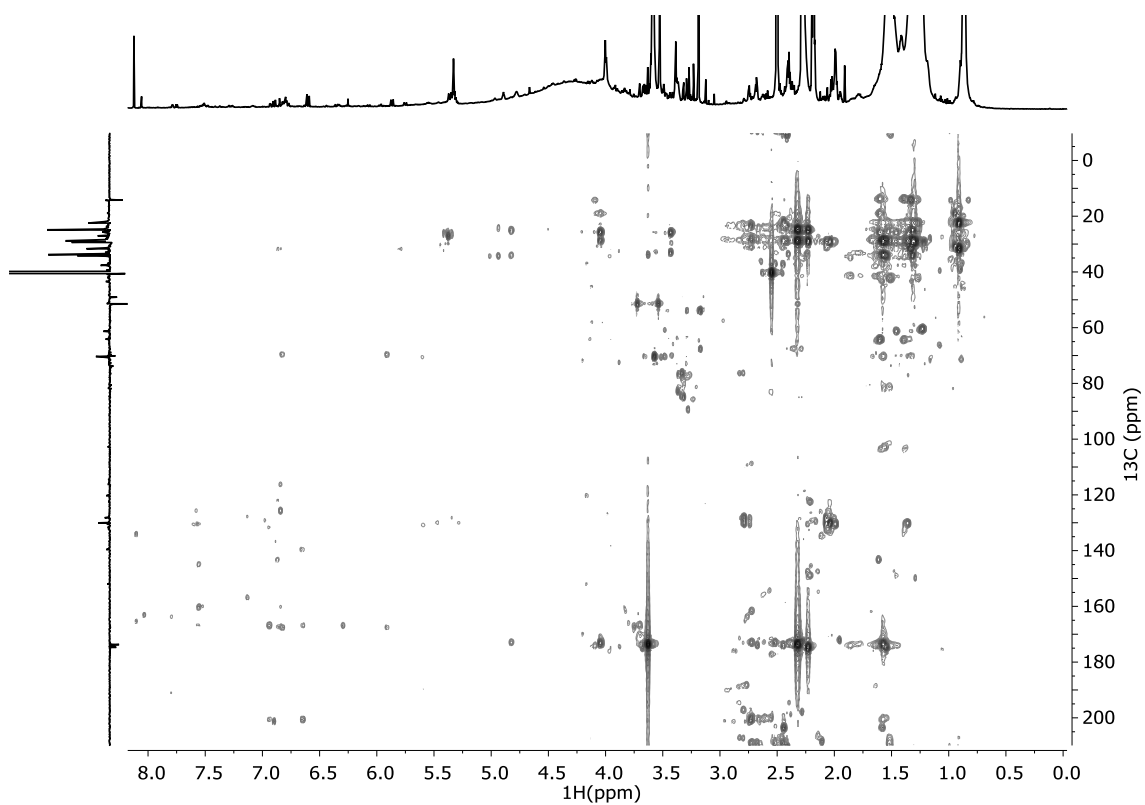


Figure S29- 2D ^1H - ^{13}C HMBC-NMR spectrum (Heteronuclear Multiple Bond Coherence) of COM4^{S} after 2 hours of hydrolysis using 0.1M NaOCH_3 upon Cutin from $\text{POM}^{\text{III-IV}}$.

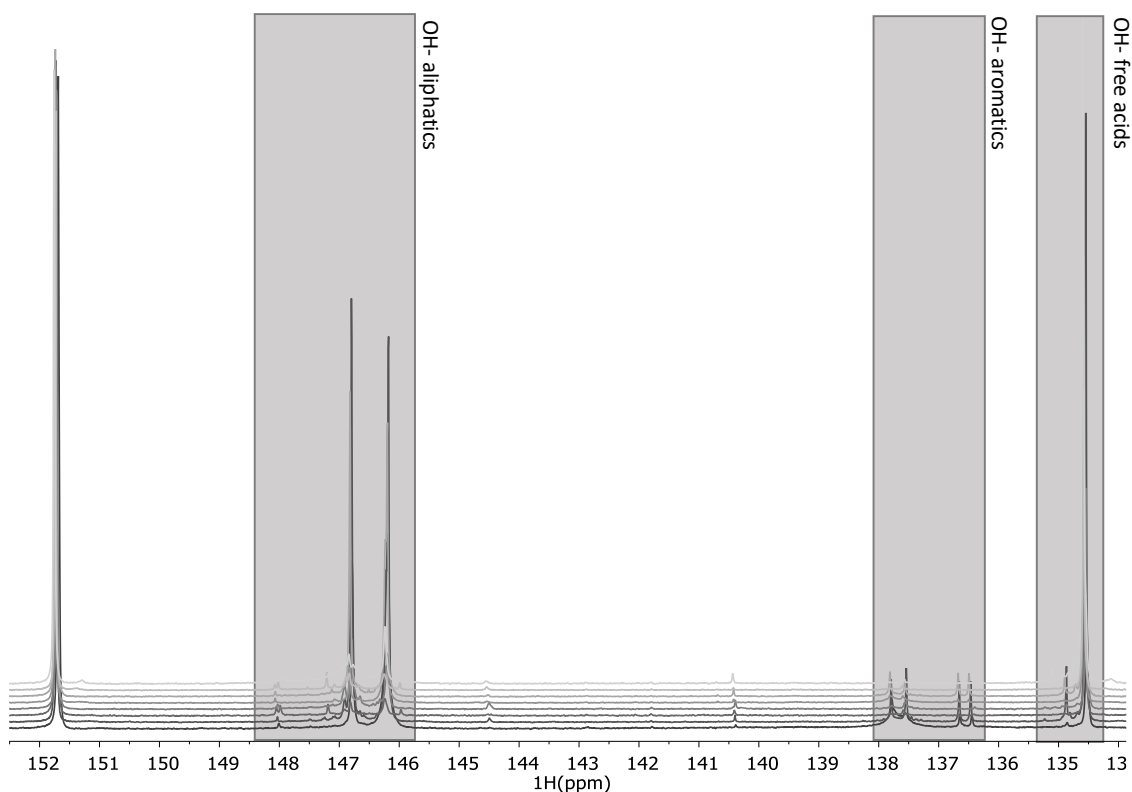


Figure S30- ^{31}P NMR spectra of COMs. The regions highlighted were used to quantify the OH-aliphatics, OH-aromatics and OH-free acids.

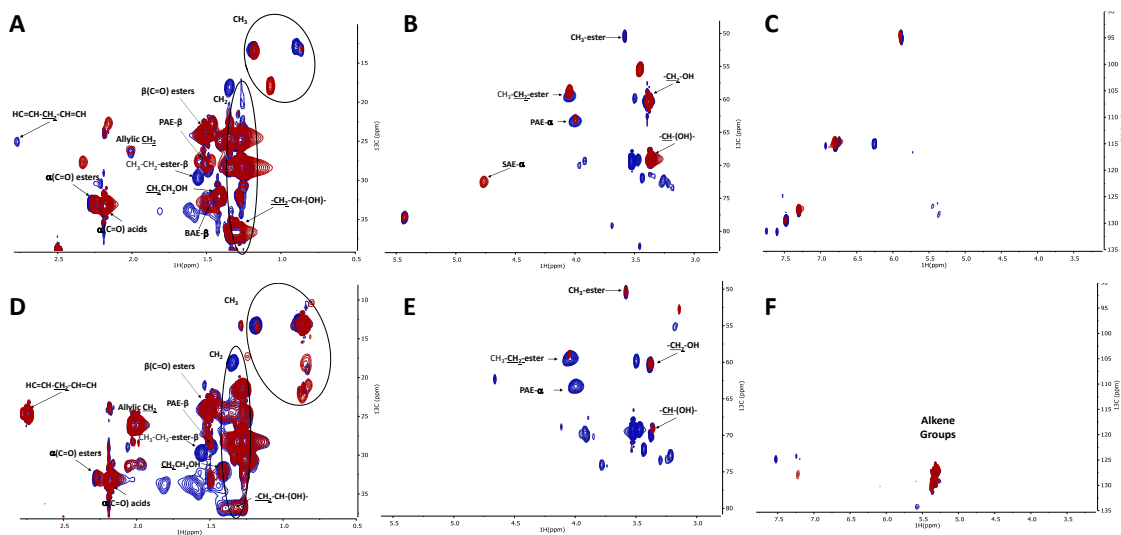


Figure S31- 2D- ^1H ^{13}C - HSQC spectral characterization peels (A,B,C) and seed's (D,E,F) hydrolysates in aliphatics (A,D) glycerol CH-Acyl (B,E) and aromatics (C,F) region. Blue color stands for the soluble fraction and red color stands for the precipitated fraction. Some assignments (unlabelled) are uncertain or unidentified.

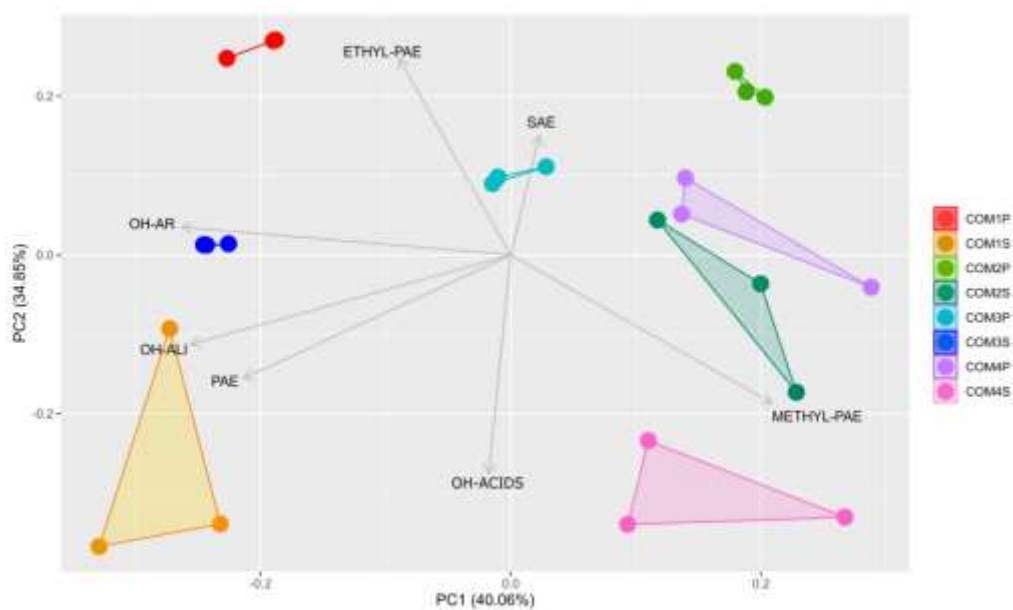


Figure S32- Principal Component Analysis (PC1;PC2) and the PCA loadings of the NMR features of COM's

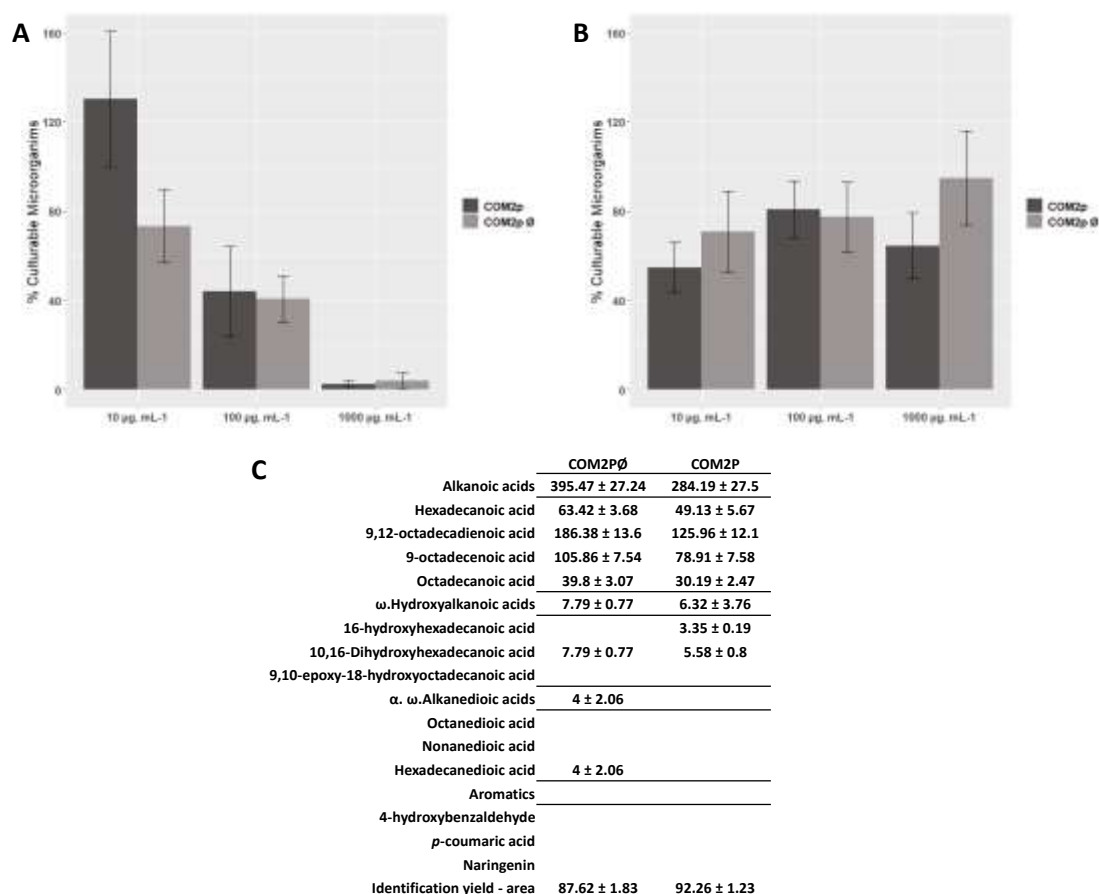


Figure S33- Antimicrobial activity comparing an oligomeric fraction with ethyl esters (COM2p) and one without ethyl esters (COM2pØ) in both *S. aureus* (A) and *E. coli* (B). Pairwise *t*-tests comparisons were used to identify significant differences between COM samples ($p < 0.05$) and the results showed no statistical difference between the samples ($n.s P > 0.05$). (C) GC-MS quantitative analysis of monomeric constituents of COM2^P and COM2^PØ.

Table S2 - Quantitative analysis of the constituents of COM's by GC-MS. Results are given as mg of compound per g of starting material. The identification yields are indicated below and represent the ratio between the identified peak area and the total area of peaks in the chromatogram. Monomers that were not detected in a specific sample are labelled as n.d.

	COM1 ^P		COM1 ^S		COM2 ^P		COM2 ^S	
	Non-hydrolysed	Hydrolysed	Non-hydrolysed	Hydrolysed	Non-hydrolysed	Hydrolysed	Non-hydrolysed	Hydrolysed
Alka(e)noic acids	141.87 ± 2.94	48.17 ± 7.49	57.54 ± 1.49	26.1 ± 3.31	284.19 ± 27.5	339.63 ± 40.61	244.36 ± 7.17	203.23 ± 11.79
Hexadecanoic acid	32.43 ± 0.57	8.4 ± 0.85	14.44 ± 0.37	6.94 ± 0.81	49.13 ± 5.67	52.94 ± 2.6	53.33 ± 1.61	37.73 ± 1.8
9,12-octadecadienoic acid	42.36 ± 1.62	21.18 ± 5.99	15.05 ± 0.16	6.89 ± 1.37	125.96 ± 12.1	170.7 ± 39.13	81.11 ± 2.41	86.01 ± 4.96
9-octadecenoic acid	37.18 ± 0.81	12.8 ± 1.02	14.07 ± 0.37	5.4 ± 0.7	78.91 ± 7.58	84.87 ± 7.7	61.7 ± 1.67	53.09 ± 3.6
Octadecanoic acid	29.91 ± 0.6	5.79 ± 0.57	13.98 ± 0.7	6.86 ± 0.84	30.19 ± 2.47	31.12 ± 3.24	48.23 ± 1.56	26.4 ± 2.04
ω-Hydroxyalkanoic acids	211.42 ± 9.3	288.36 ± 21.94	196.52 ± 45.02	257.14 ± 34.99	6.32 ± 3.76	110.21 ± 15.63	111.15 ± 3.99	182.86 ± 10.33
16-hydroxyhexadecanoic acid	15.76 ± 0.29	10.6 ± 1.13	13.73 ± 0.46	5.32 ± 0.6	3.35 ± 0.19	14.35 ± 0.56	21.71 ± 0.72	18.16 ± 1.39
10,16-Dihydroxyhexadecanoic acid	178.2 ± 8.73	263.24 ± 20.64	163.52 ± 42.1	234.11 ± 32.61	5.58 ± 0.8	82.03 ± 14.78	89.44 ± 3.36	156.75 ± 7.66
9,10-epoxy-18-hydroxyoctadecanoic acid	17.47 ± 0.55	14.52 ± 1.35	19.27 ± 2.67	17.7 ± 2.49	n.d.	13.83 ± 0.48	0 ± 0	23.86 ± 0.52
α, ω-Alkanedioic acids	10.2 ± 1	5.54 ± 2.11	22.06 ± 0.83	18.35 ± 4.48	n.d.	8.27 ± 4.31	10.66 ± 0.63	51.85 ± 1.97
Octanedioic acid	n.d.	n.d.	2.88 ± 0.17	1.58 ± 0.36	n.d.	n.d.	n.d.	n.d.
Nonanedioic acid	n.d.	1.06 ± 0.04	19.19 ± 0.9	16.77 ± 4.12	n.d.	3.68 ± 0.13	10.66 ± 0.63	39.49 ± 0.9
Hexadecanedioic acid	10.2 ± 1	4.83 ± 2.07	n.d.	n.d.	n.d.	6.98 ± 0.61	n.d.	12.36 ± 1.33
Aromatics	3.61 ± 0.4	1.65 ± 0.5	6.07 ± 0.56	2.86 ± 1.04	n.d.	5.33 ± 0.46	15.02 ± 2.87	13 ± 0.59
4-hydroxybenzaldehyde	n.d.	0.19 ± 0.07	0.4 ± 0.02	0.23 ± 0.06	n.d.	n.d.	4.31 ± 0.2	3.77 ± 0.44
<i>p</i> -coumaric acid	0.93 ± 0.07	1.03 ± 0.13	3.66 ± 0.33	1.87 ± 0.92	n.d.	5.33 ± 0.46	9.33 ± 2.58	9.23 ± 0.19
Naringenin	2.68 ± 0.34	0.52 ± 0.41	2.01 ± 0.42	0.76 ± 0.12	n.d.	n.d.	4.23 ± 0.3	nd.
identification yield (%) . area	86.16 ± 4.38	84.04 ± 2.90	71.02 ± 3.66	80.98 ± 4.53	92.26 ± 1.23	87.16 ± 9.33	53.19 ± 2.23	67.90 ± 2.22
identification yield (%) . initial mass	36.71 ± 1.23	34.37 ± 2.75	28.22 ± 4.66	30.44 ± 3.58	29.82 ± 1.54	46.34 ± 5.48	38.25 ± 1.12	45.09 ± 2.05

Table S3 - Quantitative analysis of the constituents of COM's by GC-MS. Results are given as mg of compound per g of starting material. The identification yields are indicated below and represent the ratio between the identified peak area and the total area of peaks in the chromatogram. Monomers that were not detected in a specific sample are labelled as n.d.

	COM3 ^P		COM3 ^S		COM4 ^P		COM4 ^S	
	Non.hydrolysed	Hydrolysed	Non.hydrolysed	Hydrolysed	Non.hydrolysed	Hydrolysed	Non.hydrolysed	Hydrolysed
Alka(e)noic acids	157.8 ± 25.34	144.15 ± 12.77	11.26 ± 5.77	10.29 ± 3.08	330.37 ± 16.48	330.82 ± 43.12	98.39 ± 13.82	70.04 ± 3.51
Hexadecanoic acid	31.15 ± 15.56	35.84 ± 0.96	6.19 ± 0.33	3.47 ± 0.64	115.15 ± 9.6	145.17 ± 21.54	34.08 ± 1.23	20.5 ± 2.47
9,12-octadecadienoic acid	36.67 ± 18.36	42.09 ± 1.09	6.28 ± 0.54	2.52 ± 0.24	56.99 ± 2.52	33.72 ± 3.31	29.02 ± 6.32	15.33 ± 0.8
9-octadecenoic acid	46.56 ± 27.88	49.33 ± 13.22	n.d.	2.67 ± 0.23	94.53 ± 4.31	106.22 ± 13.75	35.29 ± 6.69	24.15 ± 1.74
Octadecanoic acid	17.12 ± 8.77	16.88 ± 0.38	6.41 ± 0.11	2.92 ± 0.49	63.7 ± 3.5	45.7 ± 5.17	n.d.	12.07 ± 0.6
ω-Hydroxyalkanoic acids	96.34 ± 6.71	309.65 ± 4.19	534.57 ± 66.16	552.52 ± 61.77	36.67 ± 4.17	187.18 ± 22.6	23.32 ± 0.51	136.08 ± 19
16-hydroxyhexadecanoic acid. tms	9.78 ± 0.41	21.82 ± 0.48	6.3 ± 0.17	3.25 ± 0.34	15.55 ± 0.72	16.94 ± 1.1	n.d.	n.d.
10,16-Dihydroxyhexadecanoic acid	65.72 ± 32.67	265.2 ± 4.39	432.75 ± 48.03	512.91 ± 53.19	21.12 ± 4.27	150.32 ± 19.98	23.32 ± 0.51	136.08 ± 19
9,10-epoxy-18-hydroxyoctadecanoic acid	7.69 ± 2.39	22.63 ± 1.23	99.3 ± 21.25	37.44 ± 7.37	n.d.	19.91 ± 1.71	n.d.	n.d.
α, ω-Alkanedioic acids	9 ± 2.85	16.11 ± 1.2	22.6 ± 4.8	153.6 ± 44.21	9.63 ± 3.83	27.81 ± 5.41	100.85 ± 4.69	219.38 ± 28.92
Octanedioic acid	n.d.	n.d.	n.d.	8.36 ± 3.1	n.d.	n.d.	13.34 ± 0.28	22.73 ± 2.85
Nonanedioic acid	3.4 ± 0.55	4.86 ± 0.5	22.6 ± 4.8	145.24 ± 41.13	6.15 ± 0.12	16.52 ± 3.91	87.51 ± 4.53	189.93 ± 24.96
Hexadecanedioic acid	7.64 ± 1.48	11.26 ± 0.72	n.d.	n.d.	6.96 ± 0.25	11.29 ± 1.54	n.d.	6.72 ± 1.43
Aromatics	3.25 ± 0.15	21 ± 1.93	8.63 ± 2.15	20.13 ± 4.32	5.92 ± 0.27	6.55 ± 0.97	8.58 ± 5.95	8.04 ± 1.52
4-hydroxybenzaldehyde	n.d.	4.15 ± 0.14	0.19 ± 0.04	2.64 ± 0.5	n.d.	n.d.	4.5 ± 0.2	3.19 ± 0.04
<i>p</i> -coumaric acid	1.14 ± 0.13	14.81 ± 1.34	2.34 ± 0.52	13.38 ± 2.55	5.92 ± 0.27	6.55 ± 0.97	7.08 ± 4.21	6.45 ± 0.53
Naringenin	1.76 ± 0.87	6.12 ± 0.54	6.1 ± 1.64	4.12 ± 1.51	n.d.	n.d.	n.d.	n.d.
identification yield (%) . area	75.47 ± 7.29	72.57 ± 6.72	79.36 ± 1.71	83.91 ± 1.22	52.02 ± 2.95	71.98 ± 0.81	42.45 ± 1.23	46.85 ± 5.27
identification yield (%) . initial mass	26.70 ± 3.43	49.09 ± 1.58	57.80 ± 7.78	73.65 ± 11.26	38.16 ± 1.77	55.23 ± 7.08	23.48 ± 1.71	43.35 ± 4.75

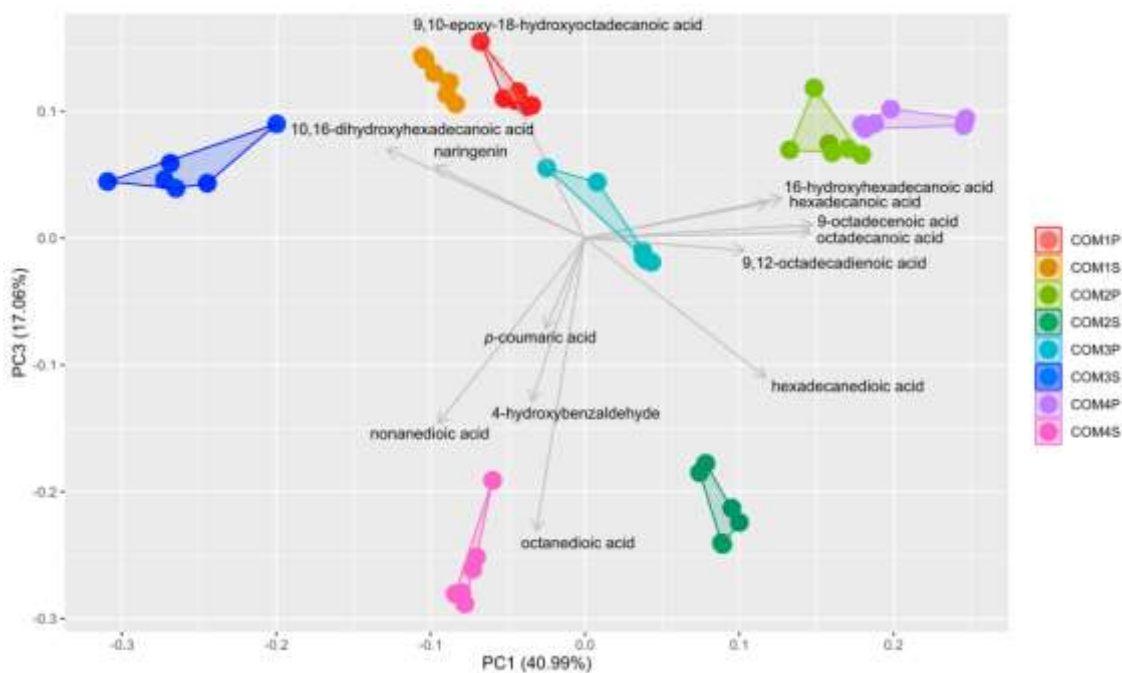
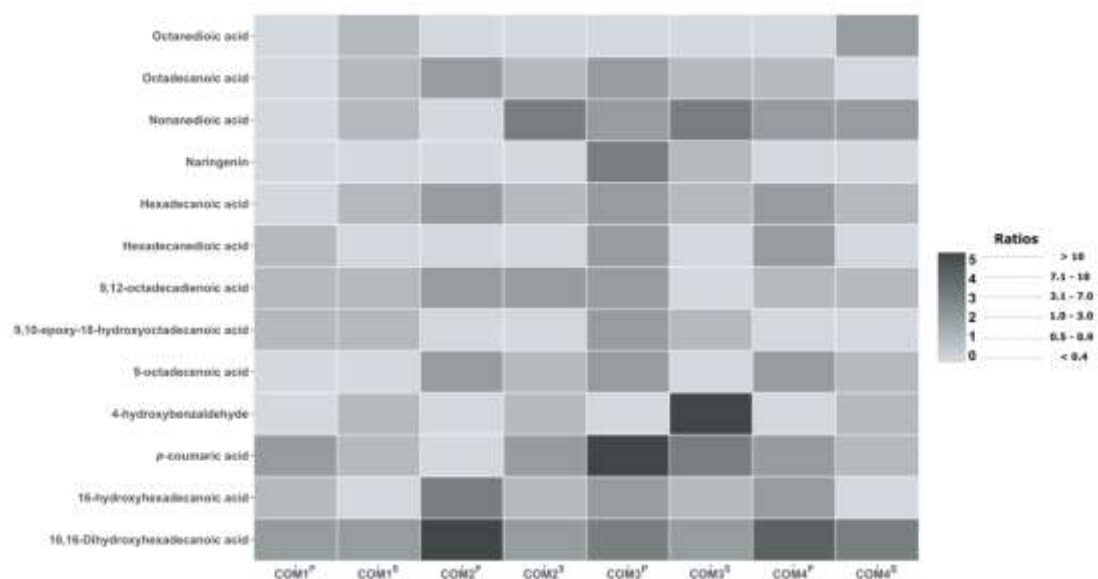


Figure S34- Principal Component Analysis (PC1;PC3) and the PCA loadings of the GC-MS data of the hydrolysable monomers identified in the COMs.

Table S4- Reported minimal inhibitory concentration (MIC)¹⁻⁵ of cutin monomers for *S. aureus* and *E. coli* and the concentration (mM) of monomers in each COM sample at 1000ug/mL, as determined by GC-MS.

	<i>S. aureus</i>	<i>E. coli</i>	COM1 ^P	COM1 ^S	COM2 ^P	COM2 ^S	COM3 ^P	COM3 ^S	COM4 ^P	COM4 ^S
	mM	mM	mM	mM	mM	mM	mM	mM	mM	mM
Hexadecanoic acid	>2		0.13	0.03	0.19	0.21	0.12	0.02	0.45	0.13
9-12-octadecadienoic acid	0.2		0.15	0.02	0.45	0.29	0.13	0.02	0.20	0.10
9-octadecenoic acid	0.4		0.13	0.02	0.28	0.22	0.16	0.00	0.33	0.12
Octadecanoic acid	>2		0.11	0.02	0.11	0.17	0.06	0.02	0.22	0.00
16-hydroxyhexadecanoic acid			0.06	0.02	0.01	0.08	0.04	0.02	0.06	0.00
10-16-Dihydroxyhexadecanoic acid			0.62	0.81	0.02	0.31	0.23	1.50	0.07	0.08
9-10-epoxy-1-hydroxyoctadecanoic acid			0.06	0.06	0.00	0.00	0.02	0.32	0.00	0.00
Octanedioic acid			0.00	0.01	0.00	0.00	0.00	0.00	0.00	0.50
Nonanedioic acid	10.6 – 42.5		0.00	0.09	0.00	0.06	0.02	0.12	0.03	0.00
Hexadecanedioic acid			0.04	0.00	0.00	0.00	0.03	0.00	0.02	0.05
4-hydroxybenzaldehyde	8.2	8.2	0.00	0.00	0.00	0.04	0.00	0.00	0.00	0.04
p-coumaric acid	0.1 - 0.8	2.7 - 6.1	0.01	0.01	0.00	0.06	0.01	0.01	0.04	0.04
Naringenin	0.7	1.5	0.01	0.00	0.00	0.02	0.01	0.02	0.00	0.00



	COM1 ^P	COM1 ^S	COM2 ^P	COM2 ^S	COM3 ^P	COM3 ^S	COM4 ^P	COM4 ^S
Octanedioic acid	-	0,5	-	-	-	-	-	1,7
Octadecanoic acid	0,2	0,5	1,0	0,5	1,0	0,5	0,7	-
Nonanedioic acid	-	0,9	-	3,7	1,4	6,4	2,7	2,2
Naringenin	0,2	0,4	-	-	3,5	0,7	-	-
Hexadecanoic acid	0,3	0,5	1,1	0,7	1,2	0,6	1,3	0,6
Hexadecanedioic acid	0,5	-	-	-	1,5	-	1,6	-
9,12-octadecadienoic acid	0,5	0,5	1,4	1,1	1,1	-	0,6	0,5
9,10-epoxy-18-hydroxyoctadecanoic acid	0,8	0,9	-	-	2,9	0,4	-	-
9-octadecenoic acid	0,3	0,4	1,1	0,9	1,1	-	1,1	0,7
4-hydroxybenzaldehyde	-	0,6	-	0,9	-	14,2	-	0,7
<i>p</i> -coumaric acid	1,1	0,5	-	1,0	13,0	5,7	1,1	0,9
16-hydroxyhexadecanoic acid	0,7	0,4	4,3	0,8	2,2	0,5	1,1	-
10,16-Dihydroxyhexadecanoic acid	1,5	1,4	14,7	1,8	4,0	1,2	7,1	5,8

Figure S35- Heatmap of the ratios of monomers (hydrolyzed /non-hydrolyzed) present in each COM. Scaled from 0 to 5; values higher than 1 means that the monomer was linked in an oligomeric structure.

Table S5- Recovery yields (%) of cutin-rich materials from pomace and production yields (%) of each COM fraction. Mean values obtained from 3 replicates and the respective standard deviation (SD) are shown.

		Yield %	Combined yield (P) + (S)
Cutin		55.1 ± 6.73	.
Sodium Hydroxyde	(S)	6.98 ± 0.00	57.2
	(P)	50.27 ± 0.40	
Sodium Methoxide	(S)	7.32 ± 3.82	7.26
	(P)	7.21 ± 4.26	
Sodium Hydroxyde (2nd Round)	(S)	5.06 ± 0.75	14.9
	(P)	9.8 ± 3.84	
Sodium Methoxide (2nd Round)	(S)	9.86	26.2
	(P)	16.36	

References

1. Zheng, C. J. *et al.* Fatty acid synthesis is a target for antibacterial activity of unsaturated fatty acids. *FEBS Lett* **579**, 5157–5162 (2005).
2. Blaskovich, M. A. T., Elliott, A. G., Kavanagh, A. M., Ramu, S. & Cooper, M. A. In vitro Antimicrobial Activity of Acne Drugs Against Skin-Associated Bacteria. *Scientific Reports 2019 9:1* **9**, 1–8 (2019).
3. Kozłowska, J., Grela, E., Baczynska, D., Grabowiecka, A. & Anioł, M. Novel O-alkyl Derivatives of Naringenin and Their Oximes with Antimicrobial and Anticancer Activity. *Molecules 2019, Vol. 24, Page 679* **24**, 679 (2019).
4. Guzman, J. D. Natural Cinnamic Acids, Synthetic Derivatives and Hybrids with Antimicrobial Activity. *Molecules 2014, Vol. 19, Pages 19292-19349* **19**, 19292–19349 (2014).
5. Chang, S. T., Chen, P. F. & Chang, S. C. Antibacterial activity of leaf essential oils and their constituents from *Cinnamomum osmophloeum*. *Journal of Ethnopharmacology* **77**, 123–127 (2001).